AD-A039 705 COLORADO STATE UNIV FORT COLLINS DEPT OF CHEMISTRY F/G 20/2
ON THE JAHN-TELLER EFFECT IN REF6.(U)
APR 77 G R MEREDITH, J D WEBB, E R BERNSTEIN N00014-75-C-1179
UNCLASSIFIED TR-10 NL

1 OF 1
ADA039 705

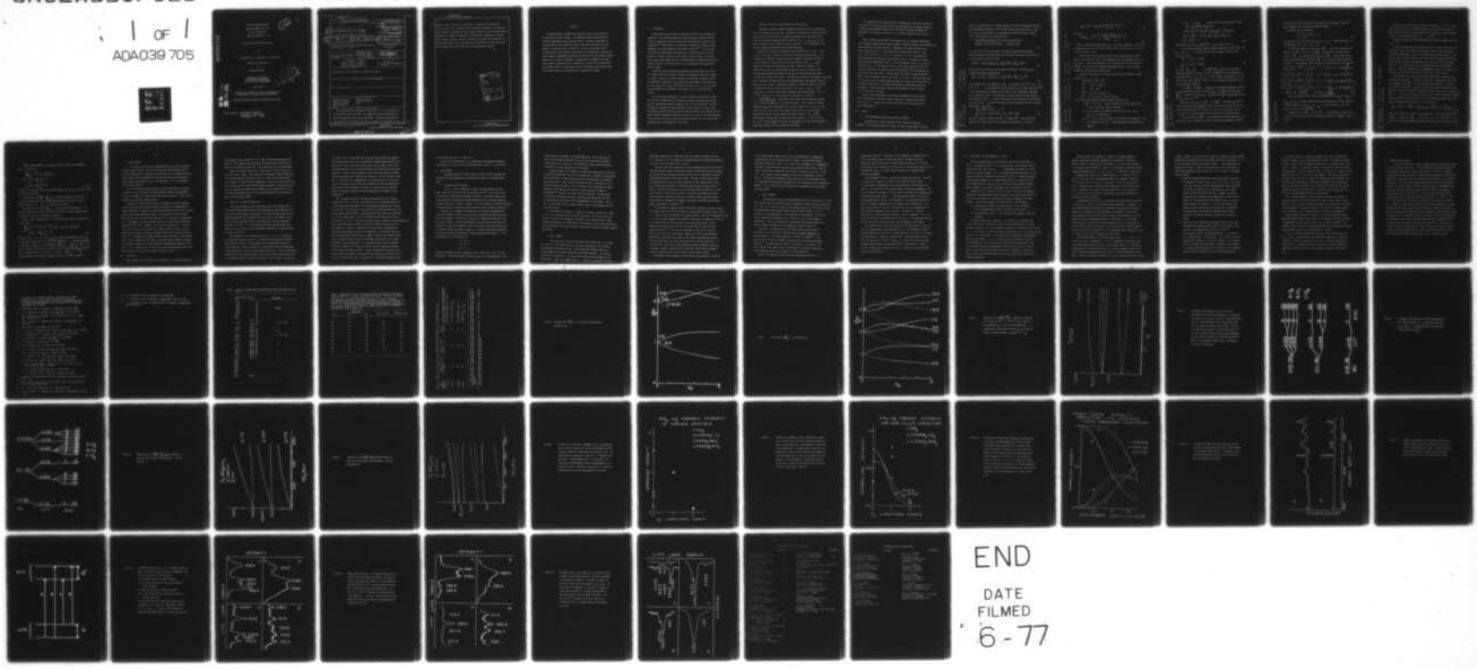

END
DATE FILMED
6-77

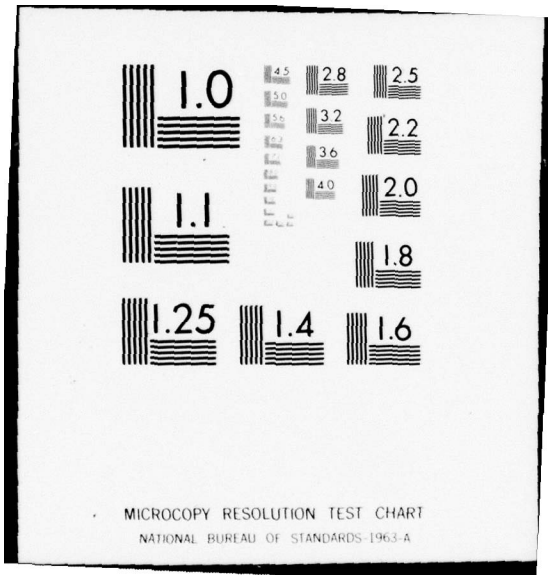
1.0
1.1
1.25
1.4
1.6
1.8
2.0
2.2
2.5
2.8
3.2
3.6
4.0
4.5
5.0
5.6
MICROCOPY RESOLUTION TEST CHART
NATIONAL BUREAU OF STANDARDS-1963-A

OFFICE OF NAVAL RESEARCH

Contract N00014-75-C-1179

Task No. NR 056-607

TECHNICAL REPORT NO. 10

"On the Jahn-Teller Effect in ReF_6"

by

G. R. Meredith*, J. D. Webb and E. R. Bernstein

Prepared for Publication

in

Molecular Physics

Department of Chemistry
Colorado State University
Fort Collins, Colorado 80523

April 1977

*Current address: Department of Chemistry
University of Pennsylvania
Philadelphia, PA 19174

UNCLASSIFIED

SECURITY CLASSIFICATION OF THIS PAGE (When Data Entered)

REPORT DOCUMENTATION PAGE	READ INSTRUCTIONS BEFORE COMPLETING FORM
1. REPORT NUMBER: 10 ✓	2. GOVT ACCESSION NO. / 3. RECIPIENT'S CATALOG NUMBER: (9)
4. TITLE (and Subtitle): (6) On the Jahn-Teller Effect in ReF_6. ✓	5. TYPE OF REPORT & PERIOD COVERED: Technical Report, / 6. PERFORMING ORG. REPORT NUMBER
7. AUTHOR(s): (10) G. R. Meredith, J. D. Webb and E. R. Bernstein	8. CONTRACT OR GRANT NUMBER(s): (15) N00014-75-C-1179 NEW
9. PERFORMING ORGANIZATION NAME AND ADDRESS: Colorado State University, Dept. of Chemistry, Fort Collins, CO 80523 ✓	10. PROGRAM ELEMENT, PROJECT, TASK AREA & WORK UNIT NUMBERS: NR 056-607
11. CONTROLLING OFFICE NAME AND ADDRESS: Office of Naval Research, Arlington, VA 22217 (12) 69p.	12. REPORT DATE: (11) April 1977 / 13. NUMBER OF PAGES: 62
14. MONITORING AGENCY NAME & ADDRESS (if different from Controlling Office): (14) TR-10	15. SECURITY CLASS. (of this report): Unclassified / 15a. DECLASSIFICATION/DOWNGRADING SCHEDULE

16. DISTRIBUTION STATEMENT (of this Report)

Approved for Public Release; Distribution Unlimited.

17. DISTRIBUTION STATEMENT (of the abstract entered in Block 20, if different from Report)

18. SUPPLEMENTARY NOTES

19. KEY WORDS (Continue on reverse side if necessary and identify by block number)

Jahn-Teller effect
molecular crystals
vibronic coupling
optical spectra
Raman scattering
crystal vibrations
ReF_6

20. ABSTRACT (Continue on reverse side if necessary and identify by block number)

New experimental and theoretical work has led to a re-evaluation of the Jahn-Teller effect in ReF_6. Low temperature neat and mixed crystal Raman and absorption spectra have been taken. The theory applicable to two Jahn-Teller active vibrations and to a Jahn-Teller molecule in a low → next page

DD FORM 1 JAN 73 1473 EDITION OF 1 NOV 65 IS OBSOLETE
S/N 0102-014-6601

UNCLASSIFIED

SECURITY CLASSIFICATION OF THIS PAGE (When Data Entered)

404992

4/B

20.

symmetry crystalline field is discussed. The main conclusions of the study are that: 1) the standard linear Jahn-Teller treatment of vibronically active modes as independent motions characterized by a given vibronic angular momentum is in general inadequate; 2) Renner-Teller (quadratic) or higher order vibronic coupling terms are important; 3) crystal field splitting of the vibronic levels is not observed; and 4) vibrational exciton band widths of the Jahn-Teller active vibrations are substantially reduced.

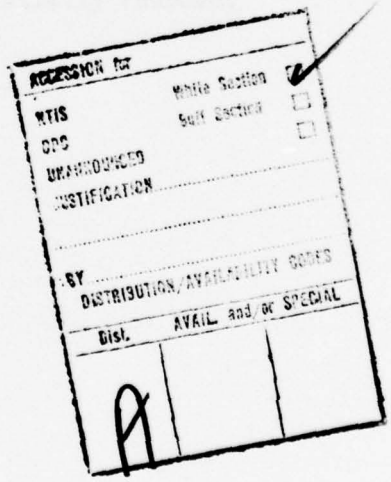

Abstract

New experimental and theoretical work has led to a re-evaluation of the Jahn-Teller effect in ReF_6. Low temperature neat and mixed crystal Raman and absorption spectra have been taken. The theory applicable to two Jahn-Teller active vibrations and to a Jahn-Teller molecule in a low symmetry crystalline field is discussed. The main conclusions of the study are that: 1) the standard linear Jahn-Teller treatment of vibronically active modes as independent motions characterized by a given vibronic angular momentum is in general inadequate; 2) Renner-Teller (quadratic) or higher order vibronic coupling terms are important; 3) crystal field splitting of the vibronic levels is not observed; and 4) vibrational exciton band widths of the Jahn-Teller active vibrations are substantially reduced.

I. Introduction

During the past two decades the Jahn-Teller effect has received much attention.[1] The infrared absorption, Raman scattering and near infrared electronic absorption spectra of ReF_6 have been discussed in terms of this interaction.[2-8] Additionally, a good deal of theoretical effort has been expended on the understanding of the effect in ReF_6.[3,9,10] In this paper we present new experimental and theoretical results which deal with the problem of vibronic coupling in the ground Γ_8 state of ReF_6. The experimental data, namely Raman and near infrared absorption spectra of ReF_6 mixed and pure crystals, form the basis for a re-evaluation of the Jahn-Teller effect in ReF_6.

Transition metal hexafluoride molecules are particularly well suited for a detailed study of vibronic coupling in degenerate states for a number of reasons: there is a series of systems to study which provides a wealth of comparative information; XF_6 systems have high symmetry, few vibrations, and only $\nu_2(e_g)$ and $\nu_5(t_{2g})$ are vibronically active in Γ_8, T_1 or T_2 states; and the systems can be studied in gas phase as well as pure and mixed crystals.

In the following discussion of vibronic coupling in ReF_6 some interesting features of Raman spectra of molecular crystals, characterized by both vibronic coupling and magnetic ordering, will also be enumerated. The data for ReF_6 are compared and contrasted with our new results for IrF_6.[11] New calculations, dealing with the vibronic coupling problem in low symmetry crystal fields and the simultaneous vibronic activity of ν_2 and ν_5, are also presented. Heavy reliance is placed on these theoretical numerical results in the final interpretation and assignment of the spectra.

II. Review of Jahn-Teller Interpretations of ReF_6 Spectra

The lowest electronic states of ReF_6 form a basis for the Γ_{8g} representation of the O_h^* double point group. According to the theorem of Jahn and Teller, any vibrations transforming as irreducible representations contained in the reduction of the antisymmetric direct product of $\Gamma_{8g} \times \Gamma_{8g}$ (a_{1g}, e_g, and t_{2g}) may participate in the intrastate vibronic coupling.[1] In the literature, each of these coupling problems has been treated separately.

Weinstock and Claassen[2] originally noticed abnormalities in the ν_2 (e_g) ~670 cm^{-1} and $\nu_5(t_{2g})$ ~300 cm^{-1} regions of the Raman spectrum of ReF_6. They attributed the observed irregular features to dynamical Jahn-Teller coupling in those modes and suggested that the diffuse nature of the $\nu_2 + \nu_3$ band observed in infrared absorption was also due to dynamical coupling. In a comprehensive review of the vibrational properties of the transition metal hexafluorides Goodman and Weinstock[3] assigned the infrared and Raman spectra in terms of the Jahn-Teller effect. The vapor phase spectra are, however, broad and, even for normal (non-Jahn-Teller active) hexafluorides, some features cannot unambiguously be assigned. Nonetheless, based on a linewidth comparison between non-Jahn-Teller active systems and ReF_6 for the $\nu_1(a_{1g}) + \nu_3(t_{1u})$, $\nu_2(e_g) + \nu_3(t_{1u})$, and ν_1 features, Jahn-Teller parameters were calculated for ν_2 and ν_5. For the ν_2 mode a large linear effect was indicated (ν_2^0 ~671 cm^{-1}, $D_2 \sim \frac{\nu_2 \text{ well depth}}{\nu_2 \text{ zero point motion}}$ ~0.09) and an additional smaller quadratic (Renner Teller) term was needed to fit the observed trends. This placed one vibronic component (Γ_{8g}) nearly degenerate with ν_1 and the other two (Γ_{6g} and Γ_{7g}) were located ca. 587 cm^{-1}; these three features then account for the observed increased breadth of the ReF_6 Raman and infrared spectra. The ν_5 Raman spectrum was assigned with a linear Jahn-Teller coupling (ν_5^0 = 297 cm^{-1} and D_5 ~.07).[5] Both assignments preserved the systematics of zero order frequencies through the chemical series of metal hexafluorides.

The Raman spectrum of ReF_6 vapor was reinvestigated later using a one-watt Ar^+ laser.[4] The broad features were fit by superposition of variable intensity, variable width components placed at the locations predicted by Goodman and Weinstock.[3] No evidence was seen for a ν_2 vibronic component in the vicinity of ν_1.

Brand, Goodman and Weinstock[5] investigated the 2μ electronic absorption band of ReF_6 in vapor phase and neat crystals. Based on intensity distributions and the frequency of the only observed ν_5 component in the Raman spectrum, two interpretations of the ν_5 linear Jahn-Teller coupling were offered. They were: $\overset{0}{\nu}_5 = 334\ cm^{-1}$, $D_5 = .31$ or $\overset{0}{\nu}_5 = 176\ cm^{-1}$, $D_5 = .42$. The latter was favored based on hot band data and selection rules for transitions to normal equivalent Born Oppenheimer states. In this assignment a level at ca. 250 cm^{-1} must be the $j_5 = \frac{1}{2}$ level while a lower $j_5 = 3/2$ level, predicted at 120 cm^{-1}, has gone unobserved. At about the same time McDiarmid[6] also investigated the same band in the vapor phase. She concluded, from rates of thermal depopulation of the vibrationless ground state, that $\overset{0}{\nu}_5 \sim 300\ cm^{-1}$. This averaged value for $\overset{0}{\nu}_5$ arises from an assumed weighted symmetrical linear Jahn-Teller splitting of vibronic levels and is in keeping with general hexafluoride vibrational systematics. She did note the problem of the selection rule for observation of the 247 cm^{-1} hot band.

The only other experimental studies which attempted to obtain information on the nature of vibronic states of ReF_6 was an infrared band contour analysis on ν_2[7]. However, these experiments were called into question by later investigators.[8]

III. Theory

A. Transition Metal Hexafluoride Vibronic Coupling

The theory of a linear Jahn-Teller (LJT) effect has been well studied.[12] This section reviews LJT theory, as well as more general vibronic

coupling, that pertains to a $\Gamma_8(O_h^*)$ electronic state of an octahedral molecule. The simultaneous treatment of the two Jahn-Teller active vibrations, $\nu_2(e_g)$ and $\nu_5(t_{2g})$, and the effect of low-symmetry crystalline fields on a Jahn-Teller active molecule are also discussed.

The Schrödinger equation for a molecule is written as

$$\mathcal{H}(\vec{p},\vec{r},\vec{P},\vec{R})\,\Psi(\vec{r},\vec{R}) = \mathcal{E}\,\Psi(\vec{r},\vec{R}) \tag{1}$$

in which $\vec{r}$, $\vec{R}$, $\vec{p}$, $\vec{P}$ are electronic and nuclear coordinates and momenta. The Hamiltonian can be partitioned into electronic and nuclear parts, and an electron-nuclear interaction term,

$$\mathcal{H}(\vec{p},\vec{r},\vec{P},\vec{R}) = \mathcal{H}_e(\vec{p},\vec{r}) + \mathcal{H}_n(\vec{P},\vec{R}) + \mathcal{H}_{en}(\vec{r},\vec{R}). \tag{2}$$

An electronic Hamiltonian can be formed by setting $\vec{R} = \vec{R}^0$, $\vec{R}^0$ being the equilibrium nuclear configuration,

$$\mathcal{H}_{el}(\vec{p},\vec{r};\vec{R}^0) = \mathcal{H}_e(\vec{p},\vec{r}) + \mathcal{H}_n(\vec{R}^0) + \mathcal{H}_{en}(\vec{r};\vec{R}^0). \tag{3}$$

The eigenfunctions and energies of $\mathcal{H}_{el}$ are denoted as $\psi_i^{el}(\vec{r};\vec{R}^0)$ and $E_i^{el}(R^0)$. If the degenerate state of interest is isolated, then $\Psi(\vec{r},\vec{R})$ can be approximated by expanding it in terms of the n degenerate components of the electronic state. This approach is often called the "Crude Adiabatic Approximation."[12f] An n x n matrix Hamiltonian can be generated by multiplying any of the n ψ_i^{*el} functions times eqn.(1) and integrating over the electronic coordinates. This gives,

$$\underline{\mathcal{H}}(\vec{P},\vec{R})\,\vec{\chi}(\vec{R}) = \mathcal{E}\,\vec{\chi}$$
$$\underline{\mathcal{H}}(\vec{P},\vec{R}) = \underline{\mathcal{H}}_n(\vec{P},\vec{R}) + \underline{\mathcal{H}}_{en}(\vec{R}) + \underline{\mathcal{H}}_e \tag{4}$$

In order to make the problem tractable, the $\underline{\mathcal{H}}_{en}(\vec{R})$ term can then be expanded in a Taylor series in the symmetry coordinates, $Q_{\Gamma\gamma}$, yielding,

ψ = Psi (lower case)
χ = Chi (lower case)
$\underline{\mathcal{H}}$ = Hamiltonian
$\underline{\Psi}$ = Psi (upper case)

$$\underline{\mathcal{H}}_{en}(\vec{R}) = \underline{\mathcal{H}}_{en}(\vec{0}) + \sum_{\Gamma,\gamma} \underline{C}^{(1)}_{\Gamma\gamma} Q_{\Gamma\gamma} + \cdots \tag{5}$$

in which

$$(C^{(1)}_{\Gamma\gamma})_{ij} = \int \psi_i^{el} \left\{ \frac{\partial \mathcal{H}_{en}(\vec{r},\vec{R})}{\partial Q_{\Gamma\gamma}} \right\}_0 \psi_j^{el} \, d\vec{r}. \tag{6}$$

Γ labels irreducible representations and γ are their components. LJT theory corresponds to retaining only the linear terms in the expansion, along with the usual elastic terms.

In the event that the linear terms are zero by group theory either because the electronic state is non-degenerate or the degeneracy is only of the Kramers' type, Born-Oppenheimer (BO) type functions can be obtained for $\Psi(\vec{r},\vec{R})$. This should be an adequate approximation for Γ_6 and Γ_7 Kramers' degenerate states in the hexafluorides.

The matrix Hamiltonian for vibronic coupling in an isolated Γ_8 state reduces to,

$$\begin{aligned}
\underline{\mathcal{H}}(\vec{r},\vec{R}) &= \underline{\mathcal{H}}^{\circ} + \underline{\mathcal{H}}' + \cdots \\
\underline{\mathcal{H}}^{\circ} &= \mathcal{H}^{\circ}_2 \underline{I} + \mathcal{H}^{\circ}_5 \underline{I} \\
\underline{\mathcal{H}}' &= \underline{\mathcal{H}}'_2 + \underline{\mathcal{H}}'_5 \\
\underline{\mathcal{H}}'_2 &= \mathcal{L}_\epsilon (q_1 \underline{\rho}_1 + q_2 \underline{\rho}_2) \\
\underline{\mathcal{H}}'_5 &= \mathcal{L}_\tau \underline{\rho}_3 (Q_1 \underline{\sigma}_1 + Q_2 \underline{\sigma}_2 + Q_3 \underline{\sigma}_3).
\end{aligned} \tag{7}$$

In the above, the following standard notation has been used:

i) $\mathcal{H}^{\circ}_2$ and $\mathcal{H}^{\circ}_5$ are the harmonic oscillator Hamiltonians for the $\nu_2(e_g)$ and $\nu_5(t_{2g})$ vibrations.

ii) q and Q denote the symmetry coordinates for the ν_2 and ν_5 vibrations, respectively

iii) $\mathcal{L}_\epsilon$ and $\mathcal{L}_\tau$ are the linear vibronic coupling parameters. They are related to the $\underline{C}^{(1)}_{\Gamma\gamma}$ (defined above) by the Wigner-Eckart theorem.

σ = lower case Sigma ∂ = partial

τ = lower case Tau ρ = lower case Rho

γ = lower case Gamma ϵ = lower case Epsilon

Σ = upper case Sigma Γ = upper case Gamma

iv) $\underline{\rho}_i$ and $\underline{\sigma}_i$ are the (4 x 4) Dirac matrices.[13] They have the following properties:

$$[\underline{\sigma}_\alpha, \underline{\sigma}_\beta] = 2i\epsilon_{\alpha\beta\gamma}\underline{\sigma}_\gamma, [\underline{\rho}_\alpha \underline{\rho}_\beta] = 2i\epsilon_{\alpha\beta\gamma}\underline{\rho}_\gamma$$
$$[\underline{\sigma}_\alpha, \underline{\sigma}_\beta]_+ = 2\delta_{\alpha\beta}\underline{I}, [\underline{\rho}_\alpha, \underline{\rho}_\beta]_+ = 2\delta_{\alpha\beta}\underline{I}$$
$$[\underline{\rho}_\alpha, \underline{\sigma}_\beta] = 0 \qquad (8)$$

Some higher order terms for $\underline{\mathcal{H}}(\vec{P},\vec{R})$ can be found in ref. 13.

In the LJT approximation, several commuting operators can be found. Let L_{2z} and $\vec{L}_5$ be the vibrational angular momenta of the ν_2 and ν_5 vibrations, then

$$\underline{\vec{J}}_5 = \vec{L}_5\underline{I} + \tfrac{1}{2}\hbar\underline{\vec{\sigma}}$$
$$\underline{J}_{2z} = L_{2z}\underline{I} + \tfrac{1}{2}\hbar\underline{\rho}_3 \qquad (9)$$

and $\underline{J}_5^2$, $\underline{J}_{5z}$, $\underline{J}_{2z}$ and $\underline{\mathcal{H}}(\vec{P},\vec{R})$ form a set of mutually commuting operators; thus the solutions of $\underline{\mathcal{H}}(\vec{P},\vec{R})$ can be labeled by the quantum numbers j_5, j_{5z} and j_{2z}. In effect these considerations (i.e., an isolated Γ_{8g} state, harmonic basis sets, etc.) reduce the problem to one of pseudo-spherical symmetry.

If the $\mathcal{H}'_5$ and $\mathcal{H}'_2$ problems are considered separately then the commuting operators are the sets $\left\{\underline{J}_5^2, \underline{J}_{5z}, \underline{\rho}_3, \underline{\mathcal{H}}'_5\right\}$ and $\left\{\underline{J}_{2z}, \underline{\sigma}_3, \underline{\mathcal{H}}'_2\right\}$, respectively. ρ_3 and σ_3 are electronic quantum numbers which take on the values ± 1.[11,12]

Numerical solutions for $\underline{\mathcal{H}}'_2$ and $\underline{\mathcal{H}}'_5$ have been found.[12e,g] Second order perturbation theory results for the case of small l_ϵ and l_z have also been obtained.[12d] However, the case in which l_ϵ and l_z are not small has not been treated previously and will be discussed here.

A secular matrix for $\underline{\mathcal{H}}'$ can be formed by using basis functions composed of ν_2 and ν_5 harmonic oscillator functions and components of the Γ_8

β = lower case Beta

γ = lower case Alpha

δ = lower case Delta

electronic functions; the explicit form need not be determined, since the matrix elements can be found using operator methods.

The basis kets are written as

$$\left| \begin{matrix} n_5 \; j_5 \; j_{5z} \; \pm \\ n_2 \; j_{2z} \qquad \pm \end{matrix} \right\rangle \tag{10}$$

in which the top ($\pm$) sign indicates that $\ell_5 = j_5 \pm 1/2$ while the bottom ($\pm$) sign indicates that $\ell_{2z} = j_{2z} \pm 1/2$.

As might be expected from the form of $\underline{\mathcal{H}'}$, only matrix elements which appear in the $\underline{\mathcal{H}'_2}$ problem or the $\underline{\mathcal{H}'_5}$ problem enter into the secular matrix for $\underline{\mathcal{H}'}$. The matrix elements for the $\underline{\mathcal{H}'_2}$ secular matrix were found by Longuet-Higgins[12e], and the $\underline{\mathcal{H}'_5}$ matrix elements were calculated by Child.[14] Above-diagonal matrix elements are gathered here for convenience:

$$\left\langle \begin{matrix} n_5 \; j_5 \; j_{5z} \; \pm \\ (n_2-1) \; j_{2z} \; - \end{matrix} \middle| \, \underline{\mathcal{H}'} \, \middle| \begin{matrix} n_5 \; j_5 \; j_{5z} \; \pm \\ n_2 \; j_{2z} \qquad + \end{matrix} \right\rangle = \left\{ (n_2 + j_{2z} + 1/2) D_2 \right\}^{1/2} \hbar \omega_5$$

$$\left\langle \begin{matrix} n_5 \; j_5 \; j_{5z} \; \pm \\ (n_2-1) \; j_{2z} \; + \end{matrix} \middle| \, \underline{\mathcal{H}'} \, \middle| \begin{matrix} n_5 \; j_5 \; j_{5z} \; \pm \\ n_2 \; j_{2z} \qquad - \end{matrix} \right\rangle = \left\{ (n_2 - j_{2z} + 1/2) D_2 \right\}^{1/2} \hbar \omega_2$$

$$\left\langle \begin{matrix} (n_5-1) \; j_5 \; j_{5z} \; - \\ n_2 \; j_{2z} \qquad \pm \end{matrix} \middle| \, \underline{\mathcal{H}'} \, \middle| \begin{matrix} n_5 \; j_5 \; j_{5z} \; + \\ n_2 \; j_{2z} \qquad \pm \end{matrix} \right\rangle = (\mp) \left\{ (n_5 + j_5 + 3/2) D_5 \right\}^{1/2} \hbar \omega_5$$

$$\left\langle \begin{matrix} (n_5-1) \; j_5 \; j_{5z} \; + \\ n_2 \; j_{2z} \qquad \pm \end{matrix} \middle| \, \underline{\mathcal{H}'} \, \middle| \begin{matrix} n_5 \; j_5 \; j_{5z} \; - \\ n_2 \; j_{2z} \qquad \pm \end{matrix} \right\rangle = (\mp) \left\{ (n_5 - j_5 + 1/2) D_5 \right\}^{1/2} \hbar \omega_5$$

in which $D_2 = \dfrac{\ell_\epsilon^2}{2 m_2 \hbar \omega_2^3}$ and $D_5 = \dfrac{\ell_\zeta^2}{2 m_5 \hbar \omega_5^3}$. (11)

Thus, the problem can be solved by diagonalizing a $[(n_{5_{max}}+1)(n_{2_{max}}+1)$ by $(n_{5_{max}}+1)(n_{2_{max}}+1)]$ matrix whose elements have been given by simple formulae. A typical value for both $n_{5_{max}}$ and $n_{2_{max}}$ is 9 which leads to a 100 x 100 secular matrix to be diagonalized.

Examples of the $\underline{\mathcal{H}'_2}$ and the $\underline{\mathcal{H}'_5}$ calculations are given in Figs. 1 and 2; an illustration of the simultaneous calculation for $\underline{\mathcal{H}'}$ is given in Figure 3.

ω = lower case Omega

Selection rules for Raman scattering are given by $\Delta j_i = 0, 1$[15]. Selection rules for an optical transition between a BO state and a LJT state depend on the vibrational angular momentum of the BO state l_i and are given in terms of the quantum numbers by $l_i = j_i \pm 1/2$[15].

Intensity calculations have been discussed by Brand, Goodman, and Weinstock.[5, 16]

In the event that the LJT approximation fails, a qualitative idea of the splitting, mixing and shifting of the vibronic levels can be obtained by considering the symmetry, in O_h^*, of the zeroth-order vibronic states. The symmetry labels of these states can be found simply by taking the direct product of the irreducible representations of the electronic and vibrational functions. This approach can be called General Vibronic Coupling (GVC) theory. Correlations between the Born-Oppenheimer states, LJT states and the GVC states are shown in Figure 4 and Figure 5 for ν_2 and ν_5 levels.

At low temperatures, the hexafluorides belong to the space group Pnma and have site symmetry C_s. Thus, it is important to determine the effect of a low symmetry field $\underline{\Phi}$ on a Jahn-Teller active molecule. Since the splitting of the electronic origin is typically an order of magnitude larger than the splitting of "normal" vibrations, only the former will be treated, i.e., $\underline{\Phi}(\vec{r})$. By using the symmetry properties (C_s) and the hermiticity of $\underline{\Phi}(\vec{r})$, a matrix Hamiltonian for the site field can be expressed in terms of certain O_h tensor operators, represented in a Γ_8 manifold, as

$$\underline{\Phi}_{C_s} = k^{A_{1g}} \underline{I} + k_\Theta^{E_g} \underline{\rho}_1 + k_\xi^{t_{2g}} \underline{\rho}_3 \underline{\sigma}_1 + k_\eta^{t_{2g}} \underline{\rho}_3 \underline{\sigma}_2 + k_\zeta^{t_{2g}} \underline{\rho}_3 \underline{\sigma}_3 . \quad (12)$$

Since the mirror plane is taken to be between the x and y axes, $k_\xi^{t_{2g}} = k_\eta^{t_{2g}}$. If $\underline{\Phi}_{C_s}$ is added to $\underline{\mathcal{H}}$, the j_5, j_{5z}, j_{2z}, (ρ_3 and σ_3) all cease to be good quantum numbers and general solutions are difficult to obtain.

Φ = upper case Phi ξ = lower case Xi η = lower case Eta
θ = lower case Theta ζ = lower case Zeta

A useful approximation is to consider the site symmetry as tetragonal (D_{4h}). In that case,

$$\underline{\Phi}_{D_{4h}} = k'^{A_{1g}}\,\underline{I} + k'^{E_g}_{\Theta}\,\underline{\rho}_1$$

and $$\left[\underline{J}_5^2\,,\,\underline{\Phi}_{D_{4h}}\right] = 0$$

$$\left[\underline{J}_{5z}\,,\,\underline{\Phi}_{O_{4h}}\right] = 0\,. \qquad (13)$$

Therefore, j_5 and j_{5z} remain good quantum numbers (j_{2z}, ρ_3, σ_3 do not), which simplifies calculations.

Calculations for $(\underline{\mathcal{H}}'_5 + \underline{\Phi}_{D4h})$ show that the crystal field (CF) splitting of the origin Δ is carried approximately, by the rest of the ν_5 vibronic levels ($\Delta \simeq \Delta'$). This is illustrated in Figure 6.

Calculations for $(\underline{\mathcal{H}}'_2 + \underline{\Phi}_{D4h})$ give much different results. In certain vibronic levels the crystal field splitting is largely quenched while in others it is not, as illustrated in Figure 7.

Another useful approximation is to assume that the field is trigonal (D_{3d}). In that case,

$$\underline{\Phi}_{D_{3d}} = k''^{A_{1g}}\,\underline{I} + k^{t_{2g}}\left(\underline{\rho}_3\,\underline{\sigma}_1 + \underline{\rho}_3\,\underline{\sigma}_2 + \underline{\rho}_3\,\underline{\sigma}_3\right)$$

and $$\left[\underline{J}_{2z}\,,\,\underline{\Phi}_{D_{3d}}\right] = 0\,. \qquad (14)$$

Therefore, ρ_3, σ_3, j_5, j_{5z} are lost as good quantum numbers and only j_{2z} remains to classify states of $(\underline{\mathcal{H}}(\vec{P},\vec{R}) + \underline{\Phi}_{D3d})$. Qualitative behavior of the $(\underline{\mathcal{H}}'_2 + \underline{\Phi}_{D_{3d}})$ and the $(\underline{\mathcal{H}}'_5 + \underline{\Phi}_{D3d})$ problems is clear: The crystal field splittings of some vibronic levels in the $(\underline{\mathcal{H}}'_5 + \underline{\Phi}_{D_{3d}})$ problem may be quenched, whereas in the case of $(\underline{\mathcal{H}}'_2 + \underline{\Phi}_{D_{3d}})$, the splitting should be reproduced throughout the entire vibronic spectrum.

B. Neat Crystal

In a neat crystal every site adapted molecular state will generate a band of crystal states. For the transition metal hexafluoride crystal structure, 4m branches (or brands) will be created from site adapted molecular levels with m (nearly) degenerate states when the levels are described by single valued representations (e.g., BO vibrations). 2m $\underline{k}$ = 0 components will be Raman allowed.[17]

For site states described by double valued representations (electronic or vibronic states of ReF_6) but retaining Kramers degeneracy (paramagnetic crystal), the details of crystal states have been discussed.[18] Again 2m $\underline{k}$ = 0 components are allowed in Raman spectra.

Discussion of single valued crystal excitations deriving from double valued site functions has been presented for magnetically ordered ReF_6.[18] Kramers degeneracy is removed in a magnetically ordered crystal and, in general, one may expect 4m nondegenerate levels. Selection rules for the various magnetic structures have also been determined. All, in general, nondegenerate 4m $\underline{k}$ = 0 components are Raman allowed for structures described by Shubnikov groups Ш_{62}^{443}, Ш_{62}^{444}, Ш_{62}^{445}, and Ш_{62}^{449} (see Figure 5, reference 18). Since each site corepresentation of the remaining groups applicable to ReF_6 crystals induces equal numbers of gerade and ungerade factor group corepresentations, only 2m $\underline{k}$ = 0 components are Raman allowed in those structures. The implication is that a doubling of the number of observed Raman components, compared to the number observed in the high temperature paramagnetic structure, could occur. It will therefore be difficult to use the low temperature neat crystal Raman spectra in discussing the vibronic coupling in ReF_6.

IV. Experimental

The experiments to determine relative intensities in the 2μm absorption

band of ReF_6 in MF_6 crystals (M = Re, W, Mo, U) have been previously presented.[18] The intensities were measured from high resolution data transferred to an optical density scale. The spectra were cut out and weighed.

Crystals for Raman studies were: ReF_6 (neat), 5% ReF_6 in TeF_6 and in UF_6, and 1% ReF_6 in MoF_6. Description of the syntheses, sample preparation and crystal growth may be found in ref. 18. Raman spectra were obtained of all samples at liquid nitrogen temperature. Spectra of the neat and TeF_6 host crystals were also obtained with samples immersed in superfluid helium. Spectral interferences made the UF_6 and MoF_6 crystal samples difficult to interpret and therefore most of the ensuing discussion will be confined to ReF_6 and 5% ReF_6/TeF_6 samples.

V. Intensities in Optical Transitions

It has been pointed out that non-BO character of the ground state of ReF_6 should induce progressions of the corresponding normal vibrations in a transition to the BO type Γ_{7g} manifold.[5] This fact has been used by Brand, Goodman and Weinstock[5] to estimate the value of D_5 in the ground Γ_8 state. Several factors conspire to make this theoretically correct procedure inapplicable for ReF_6. All of them hinge on the fact that the vapor phase spectra are very broad and to get meaningful intensities the spectra have to be taken in the solid.

The intensities of the transitions to the ν_5 n = 0, 1, 2 levels have been measured in various crystals. The results are displayed in Figure 8; normalization to the n = 1 level points out the significant variation of origin intensity. There is evidently a strong origin intensity enhancement associated with pure crystal intermolecular interactions. The origin intensity decreases with concentration showing that even at 2 mole percent concentration aggregates bring in significant intensity. The 0.3% ReF_6 in UF_6 origin

intensity is still larger than the 0.3% ReF_6 in MoF_6 intensity presumably due to the longer range of the intermolecular superexchange interactions in that host.[18] One is forced to accept the 0.3% ReF_6 in MoF_6 value as the best approximation for an infinite dilution ideal mixed crystal transition intensity. Figure 9 which reproduces curves calculated by Brand, Goodman and Weinstock, shows that reasonable D_5 values will not fit the ReF_6 in MoF_6 data. It might also be commented that our intensity points for the neat crystal do not match exactly the values which were originally determined. Possibly our higher resolution or intensity variations due to differing amounts of magnetic ordering (differing temperatures of samples) may be responsible.

One is forced to consider alternative explanations for the intense transition to the n = 1 level. One possibility is the combined effects of a static molecular displacement in this coordinate accompanied by a change of curvature of the potential. An indication of increased distortion in the ground state has been noted[18] in conjunction with the larger site splitting of ν_6 in the ground state ($\sim$10 cm^{-1}), compared to that observed in the Γ_{7g} excited level ($\sim$3 cm^{-1}). Vibrational overlap factors computed for three-dimensional oscillators with several frequency ratios are plotted as functions of the displacement in Figure 10. Behavior of the data cannot be produced with reasonable displacements or ratios of frequencies. An important feature of both the displaced oscillator and LJT scheme is that an appreciable fraction of the intensity should be found in the higher overtones of ν_5 for larger magnitudes of either mechanism. It is therefore likely that the combined effect of a dynamical LJT effect on a static (crystal induced) distortion will not cause the behavior either. Perhaps scrambling of the normal coordinates on the low symmetry site and/or vibronic coupling to other electronic states (or between these two) is responsible for the greatly enhanced trans-

ition intensity to the n = 1 level of ν_5.

Given all of these factors, it is clear that no meaningful estimate of ground state D_5 can obtain from the intensity data of the $\Gamma_7 \leftarrow \Gamma_8$ transition.

VI. Raman Spectra

The Raman spectra of a neat crystal of ReF_6 at liquid nitrogen and superfluid helium temperatures are displayed in Figure 11 and summarized in Table 1.

A. The Normal (BO) Vibrations

The ν_1, ν_3 and ν_6 features are similar to those observed in the Raman spectra of crystalline WF_6, MoF_6 and UF_6 at 77K.[17] Only slight shifts are observed in these features between 77K and 2K. These shifts may be due to the change in intermolecular interaction derivative terms which determine excitonic structure or simply to changes in the site potential functions for those coordinates due to the added exchange potential caused by magnetic ordering.[18]

Initially it is somewhat surprising that no hot bands corresponding to transitions between vibrations associated with different low energy electronic levels are observed. Consider the splitting of a degenerate electronic state by a crystal field. In the BO approximation, separate vibrational potential surfaces exist for each electronic level; two distinct molecular energy levels are thereby created, as shown in Figure 12. If these vibrational frequencies are equal in both wells (considered a good approximation for ReF_6) $\Delta = \Delta'$ and the energies of the transitions are

$$E_a = E_d = h\nu$$
$$E_b = h\nu + \Delta$$
$$E_c = h\nu - \Delta.$$

Treating the problem on only a molecular level, transitions a and d are pure vibrational. On the other hand transitions b and c are "vibroelectronic" and

have different (and weaker) scattering mechanisms. Only transitions of type a and d have been observed in ReF_6 for the normal (BO) vibrations. This discussion also applies if the splitting has been caused by magnetic interactions, as the states are still BO states.

In ReF_6 crystals at 77K, there is a significant population of electronic excitons corresponding to the 25 cm^{-1} excited state. Wavevector conservation can be fulfilled in a band-to-band transition corresponding to a molecular type d transition. These transitions would plot out a convolution of the two exciton band structures. (This is similar to the vibrational hot band technique used to map out the electronic exciton density of states of naphthalene.)[19] However, only sharp lines are observed. The implication is that these low energy electronic excitations and vibrational excitons are not bound but exist more or less independently in the crystal. That is, a $\underline{k}$ = 0 vibrational state is created without regard to the wavevector of the electronic exciton.

If the vibration of interest is subject to vibronic coupling, the simple picture just presented for BO states does not apply. All of the levels are vibronic in nature and vibrational, electronic, and "vibroelectronic" Raman scattering mechanisms (all described in a BO reference basis) along with Rayleigh scattering mechanism can apply to every transition. Hot bands are thereby observed (see below).

B. The ν_2 Region

The TeF_6 mixed crystal and the neat crystal spectra for ν_2 are shown in Figure 13. The mixed crystal is relatively concentrated (ca. 5% ReF_6) and aggregate structure may exist. The 2K ReF_6/TeF_6 spectrum shows two intense peaks and one medium peak which are clearly monomeric. The feature at 644 cm^{-1} is probably 2 ν_4 of TeF_6 while the weak features between it and the 613 cm^{-1} peak are probably the $\nu_4 + \nu_5$ and 2 ν_5 structure.[4] The very

weak peak around 590 cm^{-1} could easily be the residual hot band of the 613 cm^{-1} transition. The 77K spectrum is generated from the 2K spectrum by addition of (type c and d) hot bands with Δ ~20 cm^{-1}.

The neat crystal 2K spectrum bears strong resemblance to the mixed crystal spectrum although magnetic ordering and (minor) exciton effects are in evidence. The 77K neat crystal spectrum may also be seen to arise from the 2K spectrum, although some frequency shifts are present. The lack of definition of the 77K spectrum must be due to excitonic behavior of the vibronic levels (or to very strong phonon coupling). The band-to-band transitions which did not result in exciton band convolutions for the normal (BO) vibrations will do so in this case. It would not be realistic to speak of multiparticle crystal states resulting from the splitting of a strongly vibronic molecular state into two nearly independent excitations, one mainly electronic and the other mainly vibrational in character.[17,18]

The vibronically coupled, crystal field split, magnetically ordered crystal site model (no exciton splitting) predicts eight possible vibronic levels in the ν_2 n = 1 region. Only four features are clearly observed. The 5 cm^{-1} temperature shift of at least one peak suggests that magnetic interactions are important since the corresponding structure did not shift in the TeF_6 mixed crystal. The 2μ absorption band of the neat crystal was also observed to shift to higher energy by 5.8 cm^{-1}.[18] One can only speculate at present as to why only half of the transitions are observed. Magnons may cause line broadening; additionally, selection rules, based on the unique (nondegenerate) ordered crystal ground state, may reduce the intensity of half the transitions. It is difficult to assess this latter mechanism because the magnetic structure is unknown. However, vibroelectronic transitions should now be allowed in principle through mixing of the BO states to form vibronic states.

The important point regarding the Jahn-Teller interpretations is that at

least three vibronic features out of the four predicted for a nonmagnetic system (Figure 3) occur within a 60 cm^{-1} region. No significant intensity was observed near the ν_1 peak. If ν_2 and ν_5 are considered to be independently involved in linear vibronic coupling, one can place an upper limit to the LJT effect as that which would cause a full 60 cm^{-1} splitting: $D_2 \simeq .03$, $\nu_2^0 \sim 586$ cm^{-1}. This would be a major downward revision of the magnitude of the LJT effect. The decrease in frequency from a zero order ν_2^0 of approximately 670 cm^{-1} predicted by hexafluoride systematics[3] is not explained by such assumptions, however. This situation along with alternative assignments will be discussed more fully later.

C. The ν_5 Region

The absence of any major intensity below 200 cm^{-1} and above 80 cm^{-1} in the neat crystal spectra and the occurrence of moderately intense structure around 380 cm^{-1} lead us to reject the second set of parameters (D_5=.42, ν_5^0=176 cm^{-1}) offered by Brand, Goodman and Weinstock[5] and to adopt the first set (D_5 = .31, ν_5^0 = 334 cm^{-1}) as a starting point in the discussion of the spectra. The 230 and 380 cm^{-1} regions are assigned as j_5 = 3/2 and j_5 = 1/2 in the LJT model, respectively. The j_5 = 1/2 regions of the neat and TeF_6 mixed crystals are shown in Figure 14 and the j_5 = 3/2 regions are shown in Figure 15.

In the j_5 = 1/2 region the 413 cm^{-1} feature in the mixed crystal is assigned as 2 ν_6 of the host, in keeping with the general upward gas to crystal shift of ν_6 in these crystals (ν_6 = 197 cm^{-1} in vapor)[4,17]. The 386 cm^{-1} peak is clearly a monomeric ReF_6 peak with an associated hot band at 367 cm^{-1}. The weak 338 cm^{-1} feature is assigned as 2 ν_6 of ReF_6. The shift from the neat crystal value is attributed to the extreme sensitivity of low frequency vibrations to changes in crystal potentials.

The j_5 = 1/2 regions of the neat crystal show features due to 2 ν_6

around 330 to 350 cm^{-1}. The sharp 351 cm^{-1} component is probably part of the 2 ν_6 structure since it shows no hot band. Collapse of the two features in the 2K neat crystal to their center of gravity at 77K and the occurrence of only one peak in the TeF_6 crystal at approximately that position, indicate that the j_5 = 1/2 neat crystal structure is a magnetic and/or excitonic phenomenon.

The assignment of the j_5 = 3/2 region is much more difficult. The neat crystal peak is composed of a number of overlapping features; there is little hope of decomposing this structure without careful polarization studies. The mixed crystal 2K spectrum shows at least five components. The 207 cm^{-1} feature is assigned as the ν_6 band of the TeF_6 host in keeping with the previous comments about 2 ν_6. The intense 230 and 220 cm^{-1} peaks are most certainly two of the j_5 = 3/2 components. The structure at 246.8 and 250.7 cm^{-1} appears remarkably like the expected site splitting of ν_4 in a D_{4h} (or D_{3d}) model for the site; the intensity ratio is approximately 2:1 with the axial component raised in energy. The overall ν_4 intensity may be due to a Fermi resonance with the j_5 = 3/2 ν_5 component. It is also possible that these two features are part of the j_5 = 3/2 component structure, but as discussed in the next section, this assignment is not favored.

The important conclusion to be extracted from these spectra is that the 380 cm^{-1} region appears consistent with the j_5 = 1/2 assignment and the increased complexity of the 230 cm^{-1} region indicates it is the j_5 = 3/2 region with overlapping ν_4 structure. Treating the ν_5 splitting alone, Figure 2 fits this data with ν_5^0 ~285 cm^{-1} and D_5 ~.15. The shift of the zero order frequency downward from an expected 300 cm^{-1} is not excessive. General vibronic coupling and interaction with the ν_2 vibronic levels are possible contributing mechanisms.

VII. Discussion of the Assignment of ν_2 and ν_5

We have performed several calculations in the LJT limit for both ν_2 and ν_5. An important result of these calculations is that even for weak LJT interactions ($D_i \sim 0.05$) in the ν_2 and ν_5 coordinates, the behavior of the levels are strongly coupled. Besides the mutual quenching and shifts of the apparent zero order frequencies (the centers of the n = 1 splitting patterns which would be required in a separated coupling fit to the data), specific level repulsions occur. Both j_{2z} and j_5 are good quantum numbers and when they are equal in two closely positioned levels, the levels will repel.

Comparison of $\overset{0}{\nu_5} = 300\ cm^{-1}$ and $\overset{0}{\nu_2} = 670\ cm^{-1}$, derived from frequency systematics, with the observed peaks centered at 230, 380, 570, and 610 cm^{-1}, leads one to conclude that the apparent zero-order frequencies have been shifted. Two possible mechanisms for this shift are the following:

a) interaction of ν_2 and ν_5 vibronic levels. This is accounted for in the $\underline{\mathcal{H}'}$ secular matrix discussed in Section III A.

b) LJT approximation fails. GVC or Renner-Teller quadratic terms are important.

In the LJT limit with a coupled ν_2-ν_5 calculation, the observed data can be fit with $D_2 = 0.08$ and $D_5 = 0.266$. The calculated levels are shown in Table 2 and Fig. 3. In this assignment, the 565 cm^{-1} feature derives from the ν_5 n = 2 BO states[2], but has mixed with (and repelled) the $j_2 = 1/2$ state deriving from the ν_2 n = 1 BO states. This latter level is repelled to approximately 900 cm^{-1} (see Figures 1, 2, 3). The three peak distribution ca. 600 cm^{-1} could probably be fit with a quadratic vibronic coupling which splits the $j_2 = 3/2$ level (forcing a readjustment of the location of the $j_2 = 3/2$ LJT level). Crystal field splitting of the 565 cm^{-1} component is rejected as being inconsistent with the apparent lack of such splittings in the ν_5 components (see below).

The above possible assignment is, however, invalidated because it predicts substantial intensity (comparable to the 565 cm^{-1} feature) at 666 cm^{-1}, 855 cm^{-1}, and 950 cm^{-1}. (See Figure 3.) In fact, some intensity is observed in the 850-1000 cm^{-1} region. But assignment of the more intense feature around 980 cm^{-1} as ν_1 + (j_5 = 3/2, j_2 = 1/2; 236 cm^{-1}) is preferred.

Rejecting the overall LJT assignment based on ν_5^0 = 300 cm^{-1} and ν_2^0 = 670 cm^{-1}, we return to the assignments based on the "apparent" values of ν_5^0 (~285 cm^{-1}) and ν_2^0 (~585 cm^{-1}). The shift, $\delta = (\nu_i^0 - \bar{\nu}_i)$, particularly for ν_2, must be largely an effect of GVC (quadratic or higher order) terms. In a Γ_8 electronic state these terms may cause not only a splitting of LJT j_i levels, but also shifts of the apparent zero order vibrational frequencies via level repulsion.

Calculations in this limit, for which GVC terms may be much larger than LJT terms (e.g., for ν_2), very rapidly become intractable. A coupled ν_2-ν_5 calculation including all terms to second order for about 10 oscillators in each well, is presently being investigated for feasibility. One of the major problems with such a calculation is that it would include in its most general form nine independent parameters. Nonetheless, it can be seen qualitatively to account for the large apparent ν_i^0 shifts and the general overall observed intensity patterns. We further point out that the problem (see Section II) of an intense 247 cm^{-1} gas phase hot band (forbidden in the LJT limit) can be easily accounted for by GVC terms.

The splitting pattern of the ReF_6 mixed crystal ν_5 n = 1 and ν_2 n = 1 regions (j_i = 3/2, 2 components; j_i = 1/2, 1 component) has also been seen in the absorption spectra of IrF_6 in hexafluoride crystals.[11] In that case, the apparent ν_5^0 is approximately 225 cm^{-1}, shifted downward by about 60 cm^{-1} from an expected unperturbed value of 285 cm^{-1} (a much larger effect than in ReF_6). The LJT splitting is described by D_5 = .03 (a much smaller effect than

in ReF_6). However, a second set of IrF_6 peaks is observed at higher energies, shifted from the original set by the crystal field origin splitting ($\Delta = \Delta'$), for all observed vibrations and vibronic levels. These comparisons are summarized in Table 3. There are two possibilities for the failure to observe corresponding crystal field split ν_2 and ν_5 states in the Raman spectra of ReF_6:

1) There are approximate selection rules disallowing transitions to the upper (or lower) crystal field split levels. This could occur, for instance, if only "vibroelectronic" type transitions (see Figure 12) connected the shifted states to the lowest (crystal field split) molecular level. However, scattering mechanisms are in general quite complicated for these vibronic states.[15] The observation of hot bands in the $j_5 = 1/2$ level argues against this exclusion. Also, the low symmetry site causes a general weak mixing of states which is responsible for observation of the molecular ungerade modes in Raman scattering, and would probably do the same for the vibronic states.

2) The crystal field splitting is quenched in ReF_6 to less than the observed line widths (about 5 cm^{-1}) by the vibronic interactions. It has been shown in Section III A that the tetragonal field is strongly quenched for ν_2 LJT coupling and is preserved for ν_5 LJT coupling. For a trigonal field the behavior with respect to ν_2 and ν_5 is reversed. This argument, of course, becomes more qualitative in nature for the coupled ν_2-ν_5 system which actually exists in either of these molecules. We believe these conclusions are still nonetheless useful.

The latter possibility seems more reasonable and can be specifically applied to compare IrF_6 ν_5 modes with ReF_6 ν_5 modes. The larger LJT effect in ReF_6 ν_5 implies that a larger distortion could be created by small crystal forces. In fact, ν_6 of ReF_6 has a factor of three larger site splittings in the ReF_6 ground Γ_8 than in either the ReF_6 Γ_7 or IrF_6 Γ_8 or Γ_7 states (>10 cm^{-1} compared to 3-4 cm^{-1}). The crux of the argument is not that the distortion has to be large, but that it removes the effective electronic crystal field from the D_{4h} regime creating a vibronically quenchable splitting operator. There may be some correlation of this effect with the nearly factor of two larger splitting of IrF_6 electronic Γ_8 levels over that of ReF_6, but the details of the wavefunctions have not been examined.

The ν_2 regions presents a difficult problem, because LJT coupling is clearly a smaller total effect than any GVC terms. Since ν_2 has not been observed in IrF_6, no direct comparison between the two molecules can be made. It would appear as though the large GVC or RT terms for ν_2 quench crystal field splitting in $n_2 \neq 0$ vibronic levels for fields of any symmetry.

Again assuming validity of separate ν_2-ν_5 vibronic quenching effects, these data taken together imply that the Γ_8 ground state of ReF_6 experiences a predominantly t_{2g}-like crystal field, IrF_6 Γ_8 states experience a predominantly e_g-like crystal field, and strong GVC terms are capable of quenching electronic crystal field interactions in Γ_8 states.

Finally, similarity between neat and mixed crystal Raman spectra for ReF_6 ν_2 and ν_5 is worth noting with regard to the quenching of electronic operators. In other hexafluorides the ν_2 and ν_5 exciton band widths are roughly 20 cm^{-1}. Apparently exciton interactions are almost completely quenched by vibronic coupling. This coupling is greater in ReF_6 than in IrF_6.

VI. Summary and Conclusions

It has been shown with a series of Raman and optical absorption spectra of neat and mixed crystals that: 1) the technique of measuring intensities of vibrational progressions in absorption spectra of crystals is possibly misleading and for ReF_6 unfruitful in determining the magnitude of Jahn-Teller coupling; 2) increased resolution, increased molecular density, and reduction of symmetry in the solid have allowed more detailed views of the ReF_6 Raman spectrum; 3) splittings due to vibronic coupling in the ν_2 mode appear small. A D_2 value less than .03 seems necessary with $\nu_2^0 \sim 586$ cm^{-1}, and there is a strong Renner Teller or GVC shift in ν_2; 4) the major splitting of the ν_5 structure is fit by a linear Jahn-Teller effect with $D_5 = .15$ and $\nu_5^0 = 285$ cm^{-1}. The small shift of ν_5^0 may be due largely to the vibronic coupling in the ν_2 modes; 5) crystal field splittings have not been observed in the upper vibronic levels and the effect has been discussed in terms of molecular distortion and the vibronic quenching of the low symmetry crystal field potential; 6) although crystal perturbation affects the details of the vibronic coupling, the similarity of the crystal and vapor spectra require reinterpretation of the vapor spectra in keeping with the above conclusions; 7) several consequences of the low lying electronic level, vibronic activity, and magnetic ordering of ReF_6 have been observed in the crystal Raman spectra; and 8) vibronic activity effectively quenches the ν_2 and ν_5 exciton structure.

1. R. Englman, "The Jahn-Teller Effect in Molecules and Crystals", (Wiley, 1972); F. S. Ham, "Jahn-Teller Effects in Electron Paramagnetic Resonance Spectra," in Electron Paramagnetic Resonance, Ed. S. Geschwind (Plenum Press, New York, 1972); M. D. Sturge, Sol. State Phys., 20, 91 (1967).

2. B. Weinstock and H. H. Claassen, J. Chem. Phys.,31, 262 (1959).

3. G. L. Goodman and B. Weinstock, Adv. Chem. Phys., 9, 169 (1965).

4. H. H. Claassen, G. L. Goodman, J. H. Holloway and H. Selig, J. Chem. Phys., 53, 341 (1970).

5. J. C. D. Brand, G. L. Goodman and B. Weinstock, J. Mol. Spec., 38, 449 (1971).

6. R. McDiarmid, J. Mol. Spec., 38, 495 (1971).

7. I. W. Levin, S. Abramowitz and A. Muller, J. Mol. Spec., 41, 415 (1972).

8. R. S. McDowell and L. B. Asprey, J. Mol. Spec., 45, 491 (1973).

9. M. S. Child and A. C. Roach, Mol. Phys., 9, 281 (1965).

10. A. A. Kiseljou, J. Phys. B, 2, 270 (1969).

11. E. R. Bernstein and J. D. Webb, to be published.

12. a) H. A. Jahn, E. Teller, Proc. Roy. Soc., A161, 220 (1937).

    b) H. A. Jahn, Proc. Roy. Soc., A164, 117 (1938).

    c) W. Moffitt, A. D. Liehr, Phys. Rev, 106(6), 1195 (1957).

    d) W. Moffitt, W. Thorson, Phys. Rev., 108(5), 1251 (1957).

    e) H. C. Longuet-Higgins, U. Optik, H. M. L. Price and R. A. Sack, Proc. Roy. Soc., A244, 1 (1958).

    f) H. C. Longuet-Higgins, Adv. Spec., 2, 429 (1961).

    g) W. Thorson, W. Moffitt, Phys. Rev., 168(2), 362 (1968).

13. R. Englman, "The Jahn-Teller Effect in Molecules and Crystals", (Wiley, 1972), p. 81.

14. M. S. Child, J. Mol. Spec., 10, 357 (1963). NOTE: A correction of a matrix element has been made.

15. M. S. Child, Phil. Trans. Roy. Soc., 255A, 1050 (1962).

16. J. C. D. Brand, G. L. Goodman and B. Weinstock, J. Mol. Spec., 37, 464 (1971).

17. E. R. Bernstein and G. R. Meredith, to be published.

18. E. R. Bernstein and G. R. Meredith, J. Chem. Phys., 64, 375 (1976).

19. S. D. Colson, D. Hanson, R. Kopelman and G. W. Robinson, J. Chem. Phys., 48, 2215 (1968).

Table 1. Summary of Raman Spectra of Neat ReF_6 Crystals taken Near 77K and 2K.

Stokes Shift (cm^{-1}) 77K	2K	Assignment
18.4		phonons
25.6		
29.9		
35.4		
49.2		
65.4		
82.9		
167		ν_6
180		
	227.4	ν_5 (j = 3/2)
232.4		
	234.0	
256.5	263.3	ν_4
350.5	335.9	2 ν_6
	350.9	
362.3	378.2	ν_5 (j = 1/2)
386.5	396.1	
541.5		ν_2
558.2	558.4	
	569.7	
579.9	580.3	
613.9	618.9	
656.9	657.1	ν_3
681.1	678.6	
687.1	684.2	
701.9	701.6	
755.3	755.0	ν_1
839		
868		
959		
992		
994.5		
1087		
1164		
1214		
1508.4	1508.6	2 ν_1

Table 2. Approximate relative intensities of Raman transitions in the lowest vibronic levels of a $\Gamma_8 \times (e_g, t_{2g})$ Jahn-Teller system. $C^2(n_2,n_5)$ are squared coefficients in the eigenvector expansion, which uses ν_2 and ν_5 harmonic oscillator functions and Γ_8 electronic functions as a basis. This approximation assumes that the only Raman scattering mechanism of importance is the usual $n = 0 \rightarrow n = 1$ mechanism based on the B.O. and harmonic oscillator approximations. The parameter values are $D_2 = 0.08$, $D_5 = 0.266$, $\nu_2^0 = 670\ cm^{-1}$, $\nu_5^0 = 300\ cm^{-1}$. (See text for further discussion.)

	eigenvectors			
$\nu(cm^{-1})$	j_5	j_2	$C^2(n_5=1, n_2=0)$	$C^2(n_5=0, n_2=1)$
0	1/2	1/2	--	--
236	3/2	1/2	.62	0
376	1/2	1/2	.30	.13
565	1/2	1/2	.10	.12
612	1/2	3/2	0	.65
666	3/2	1/2	.11	0
811	3/2	1/2	.00	0
855	1/2	1/2	.10	.14
950	1/2	1/2	.07	.30
960	1/2	3/2	0	.10

Table 3. Summary of $\nu_2(e_g)$ and $\nu_5(t_{2g})$ Vibronic Coupling Effects in Γ_8 States--ReF_6 and IrF_6

MODE (MOLECULE)	MAXIMUM SPLITTING (cm^{-1})	SHIFT $(\nu_i^o-\bar{\nu})=\delta$ (cm^{-1})	CFS(Δ') (cm^{-1})	QUALITATIVE COMMENTS AND CONCLUSIONS[a,b]
ν_2 (IrF_6)	--	--	--	Not observed--small LJT or GVC
ν_5 (IrF_6)	40	65	42	$\Delta=\Delta'$; GVC>LJT; $\Phi(\vec{r})\sim\Phi_{D_{4h}}$
ν_2 (ReF_6)	60	85	<5	$\Phi(\vec{r})$ quenched; GVC > LJT
ν_5 (ReF_6)	170	15	<5	LJT>GVC; $\Phi_{D_{4h}} << \Phi_{D_{3d}}$

a. In these comparisons it has been assumed that the totally symmetric parts of each potential function are either small or zero. Therefore, only splitting terms, not gas-to-crystal shift terms, are rigorously compared.

b. Crystal field expectation values are more fully discussed in the text. It is assumed that ν_2-ν_5 behavior with respect to $\Phi(\vec{r})$ can be approximated separately.

Figure 1. Eigenvalues of $\mathcal{H}_2'$ as a function of the coupling parameter, D_2.

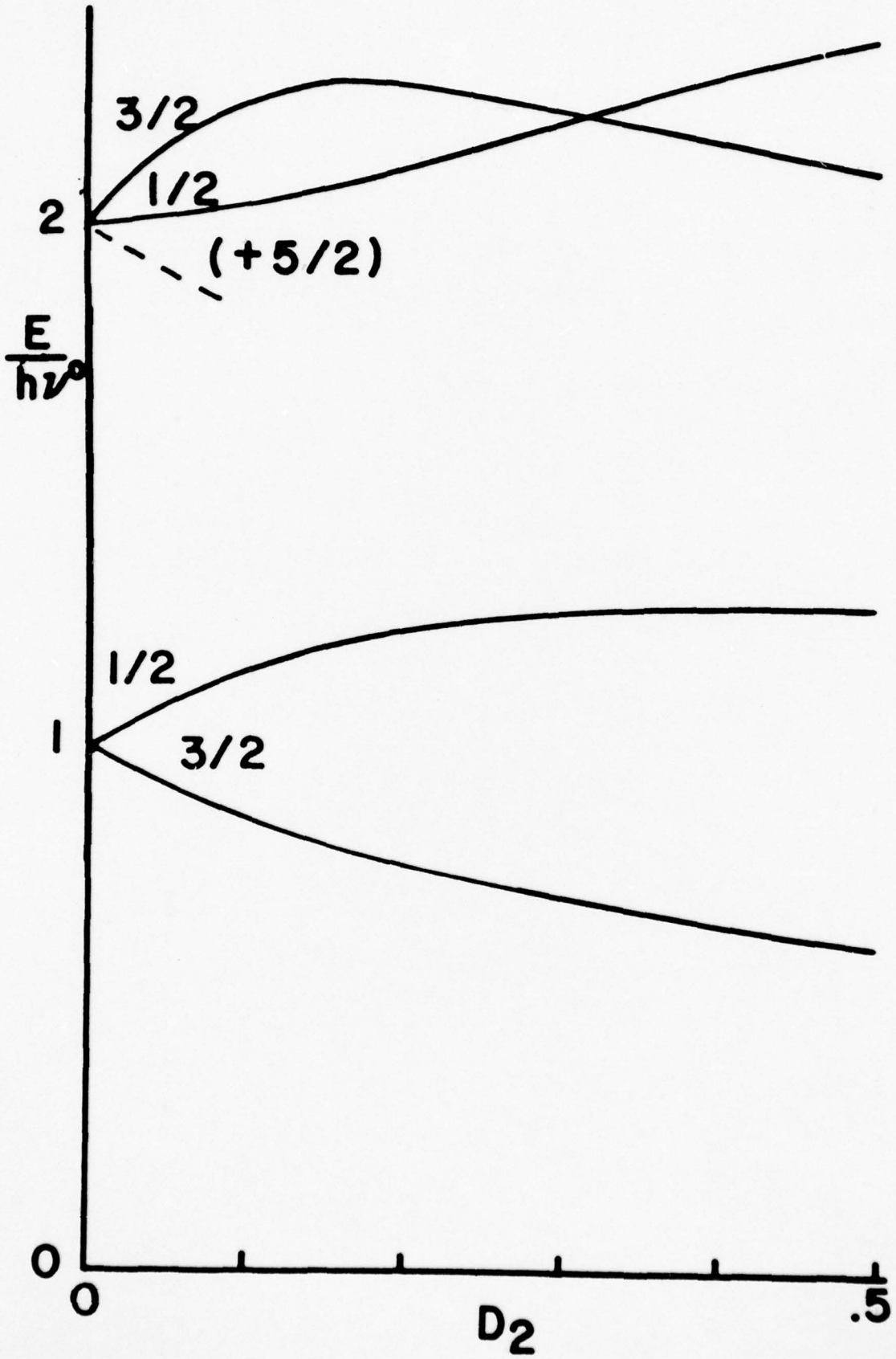
3/2
1/2
2
(+5/2)
E/hν°
1/2
1
3/2
0
0
D2
.5

Figure 2. Eigenvalues of $\mathcal{H}_5'$ as a function of D_5.

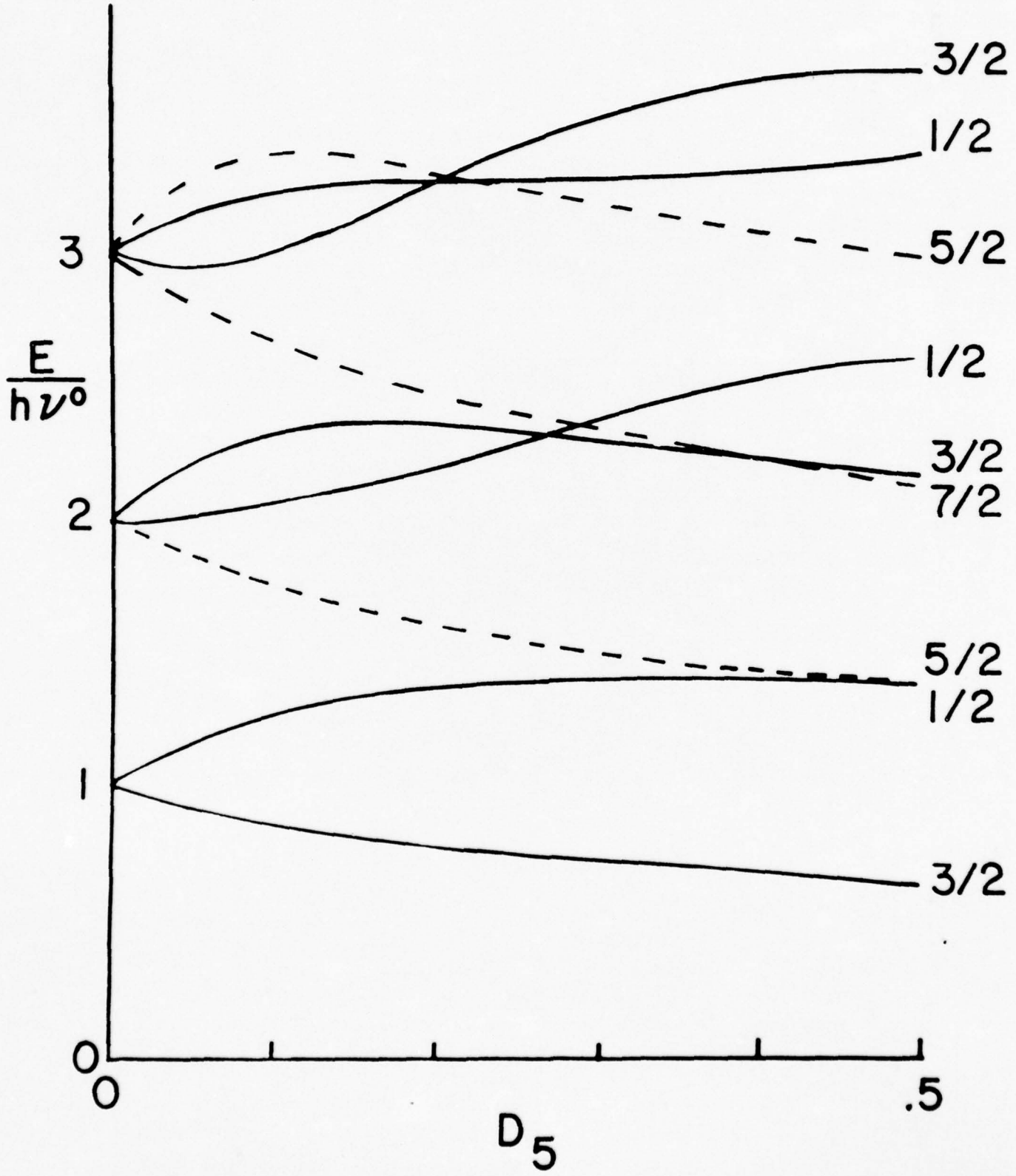
3/2
1/2
5/2
3
E
hν°
1/2
3/2
7/2
2
5/2
1/2
1
3/2
0
0
.5
D5

Figure 3. Eigenvalues of the $\{\mathcal{H}_2' + \mathcal{H}_5'\}$ problem as a function of D_5 with $D_2 = 0.08$, $\nu_2^0 = 670\ cm^{-1}$ and $\nu_5^0 = 300\ cm^{-1}$. The unobserved $j_5 = 5/2$ level is not shown here. α is a number that labels members of the (j_5, j_{2z}) sets with respect to energy ordering. J_2 stands for $\pm j_{2z}$.

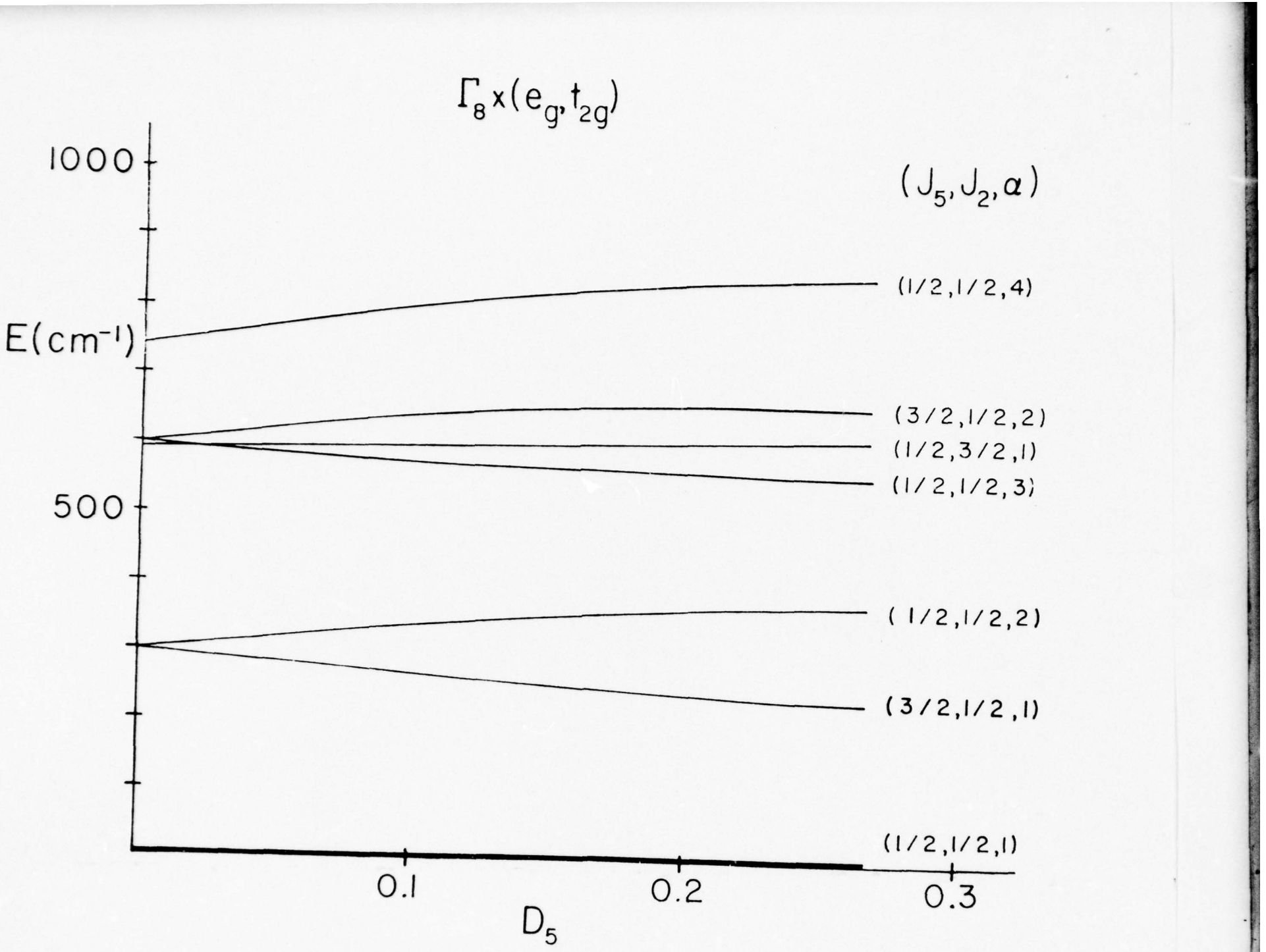
$\Gamma_8 x(e_g, t_{2g})$
1000
500
$E(cm^{-1})$
(J_5, J_2, α)
(1/2,1/2,4)
(3/2,1/2,2)
(1/2,3/2,1)
(1/2,1/2,3)
(1/2,1/2,2)
(3/2,1/2,1)
(1/2,1/2,1)
0.1
0.2
0.3
D_5

Figure 4. A schematic representation of various levels of approximation for vibronic coupling of a Γ_8 electronic state with an e_g vibration is shown. The approximations used are: Born-Oppenheimer (BO), linear Jahn-Teller (LJT), and general vibronic coupling (GVC). BO states are labeled by the number of vibrational quanta; LJT states are labeled by their vibronic angular momentum; and GVC states are labeled by irreducible representations of the octahedral double group. Degeneracies are listed in parentheses.

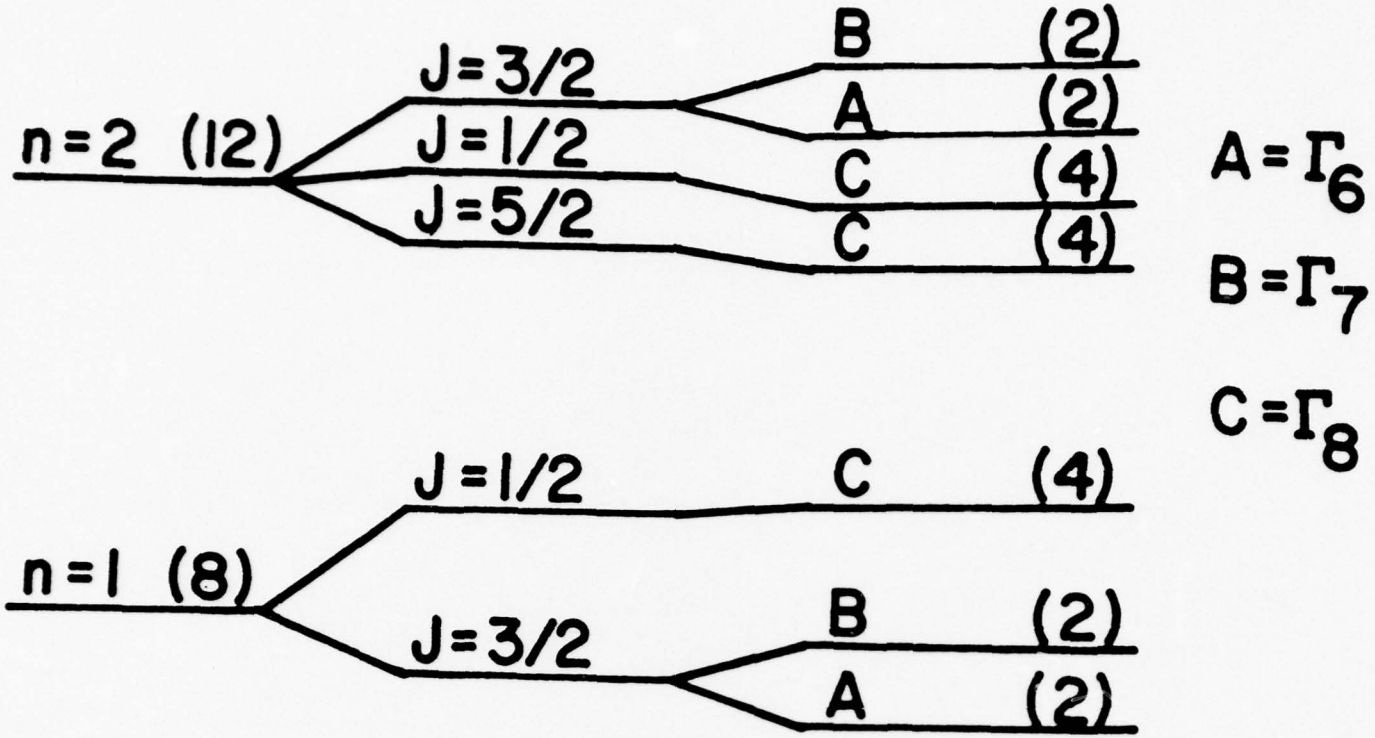
n=2 (12)
J=3/2
J=1/2
J=5/2
B (2)
A (2)
C (4)
C (4)
A = Γ6
B = Γ7
C = Γ8
n=1 (8)
J=1/2
J=3/2
C (4)
B (2)
A (2)
n=0 (4)
J=1/2
C (4)
BO
LJT
GVC

Figure 5. A schematic representation of various approximations for vibronic coupling of a Γ_8 electronic state with a t_{2g} vibration. The approximations are described in the caption to Figure 4.

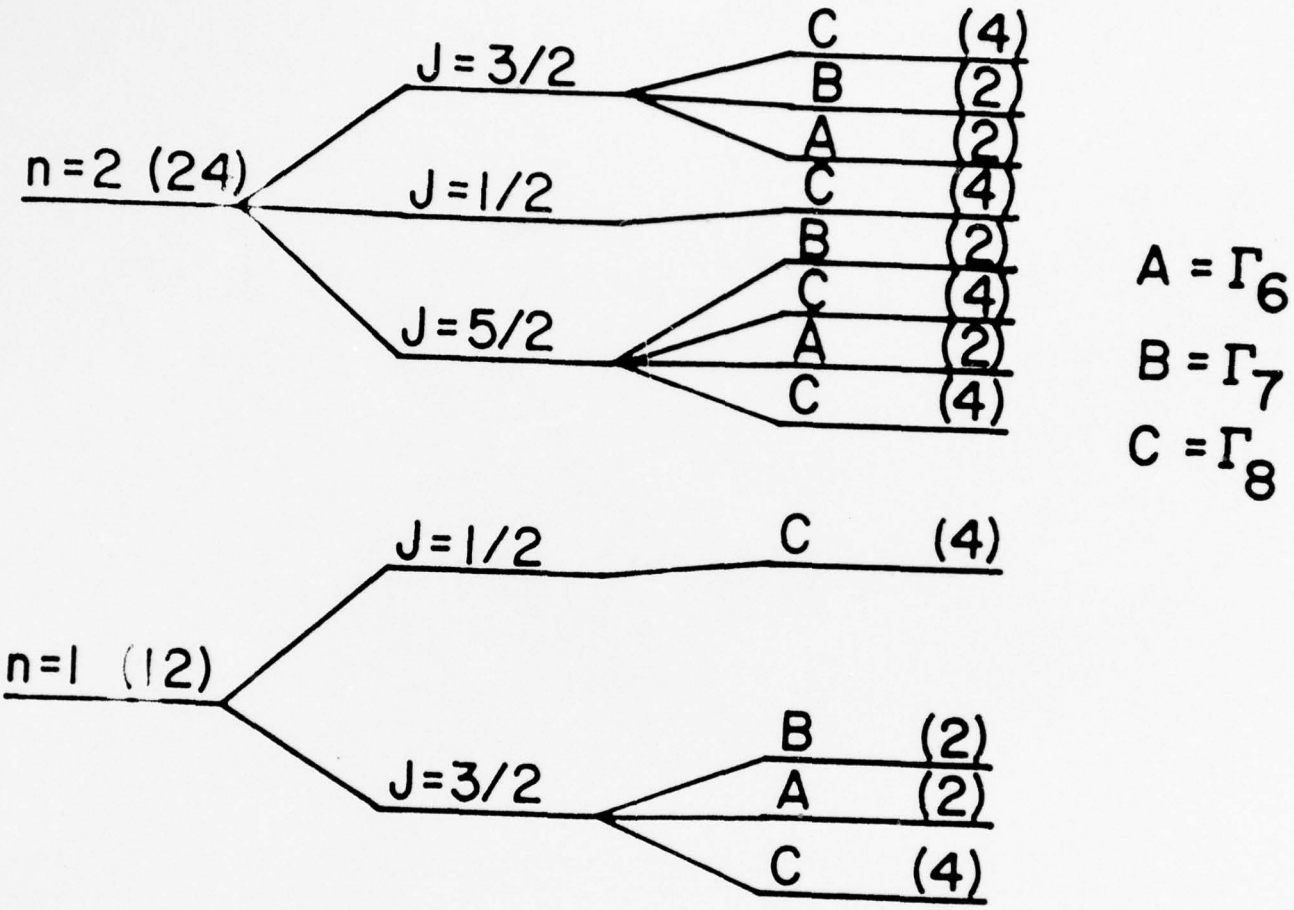
n=2 (24)
J=3/2
J=1/2
J=5/2
C (4)
B (2)
A (2)
C (4)
B (2)
C (4)
A (2)
C (4)
A = Γ6
B = Γ7
C = Γ8

n=1 (12)
J=1/2
J=3/2
C (4)
B (2)
A (2)
C (4)

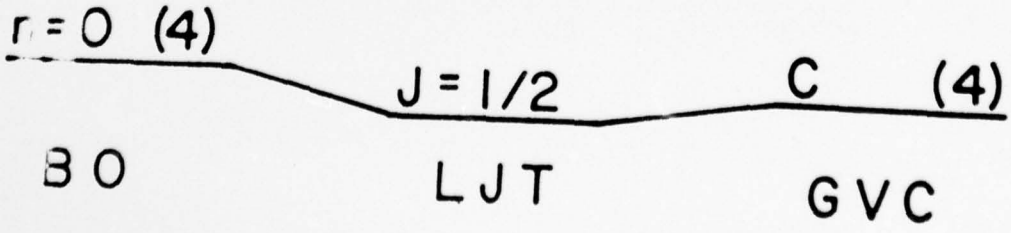
n=0 (4)
J=1/2
C (4)
B O
L J T
G V C

Figure 6. Eigenvalues of the $\{\underline{\mathcal{H}}_5' + \underline{\Phi}_{(O_h)}\}$ Hamiltonian as a function of the crystal field parameter. See text and eqn. 13.

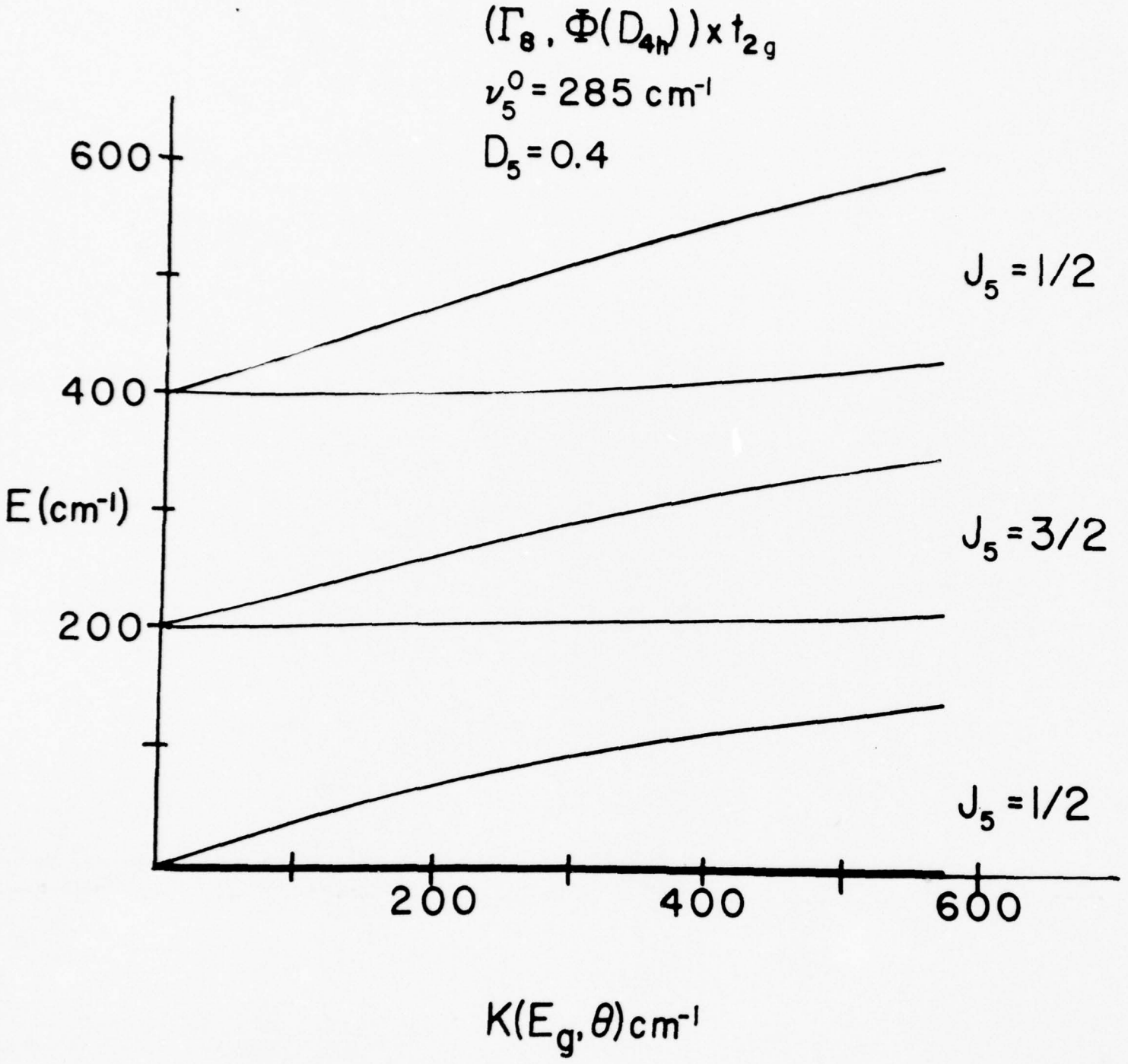
$(\Gamma_8, \Phi(D_{4h})) \times t_{2g}$
$\nu_5^0 = 285\ cm^{-1}$
$D_5 = 0.4$
600
400
200
E(cm⁻¹)
$J_5 = 1/2$
$J_5 = 3/2$
$J_5 = 1/2$
200
400
600
$K(E_g, \theta)\ cm^{-1}$

Figure 7. Eigenvalues of the $\left\{\underline{\mathcal{H}}_2' + \underline{\Phi}_{(D_{4h})}\right\}$ Hamiltonian as a function of the crystal field parameter. See text and Equation 14.

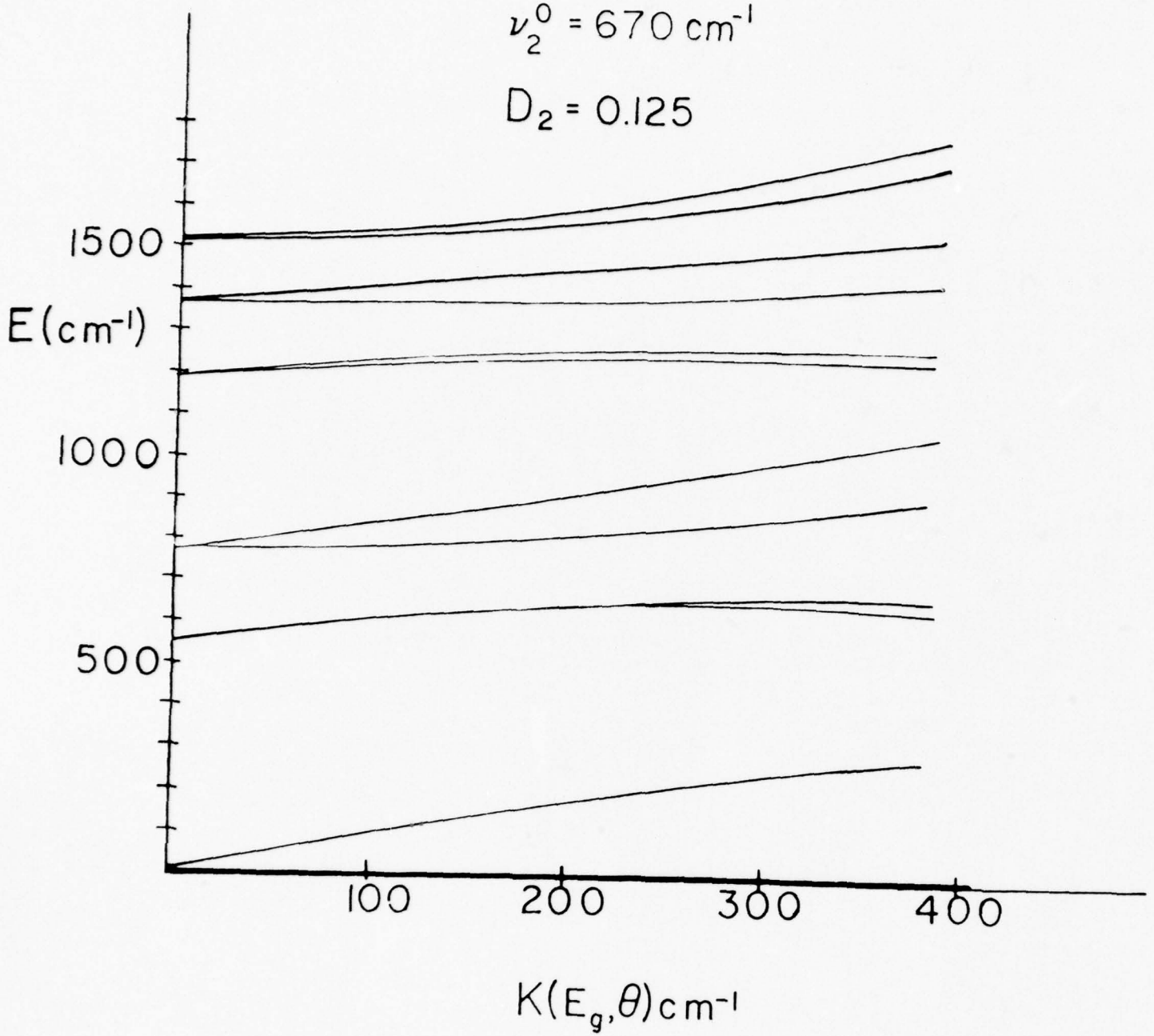
$(\Gamma_8, \Phi(D_{4h})) \times E_g$
$\nu_2^0 = 670\ cm^{-1}$
$D_2 = 0.125$
1500
E(cm⁻¹)
1000
500
100
200
300
400
K(E_g, θ) cm⁻¹

Figure 8. A plot of the intensities of members of the ν_5' progression, which is built on the origin in the 2μ absorption spectrum of ReF_6 is given for various MF_6 mixed crystals at 2K. The intensities are normalized so that the n = 1 component has unit value. The discrepancy of n = 0 intensities is an indication of intermolecular intensity enhancement as discussed in the text. The small variation of n = 2 levels is considered to be within the experimental uncertainty.

ReF_6 $n\nu_5'$ VIBRONIC INTENSITY IN VARIOUS CRYSTALS

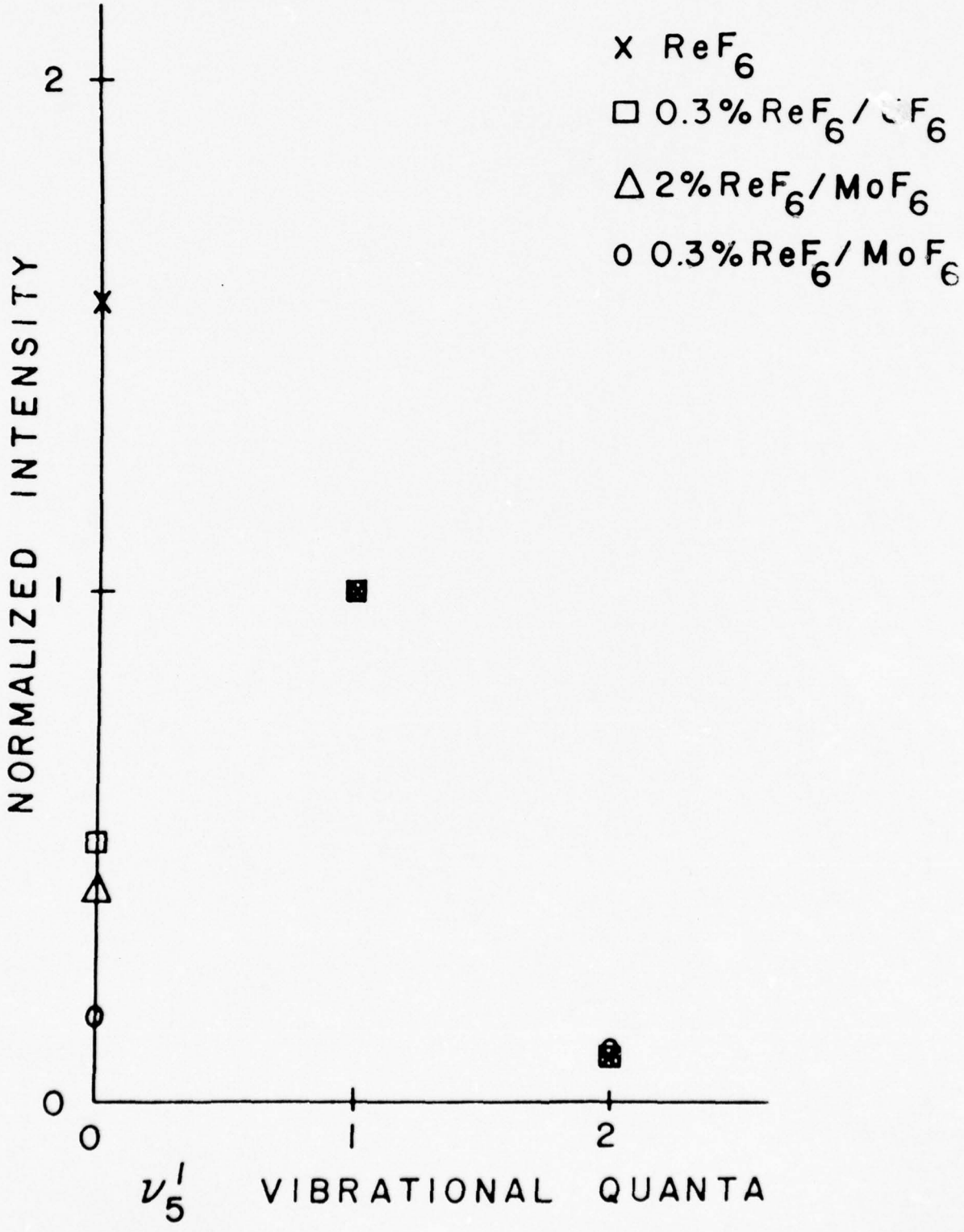

Figure 9. Intensities of members of the ν_5' progression, which is built on the origin in the 2K 2μ absorption spectra of ReF_6 in various MF_6 hosts, are compared to linear Jahn-Teller predictions. The experimental intensities are normalized to unity for the three observed components. The linear Jahn-Teller curves are reproduced from reference 5. The disagreement of experimental points (except neat crystal) with reasonable Jahn-Teller predictions is discussed in the text.

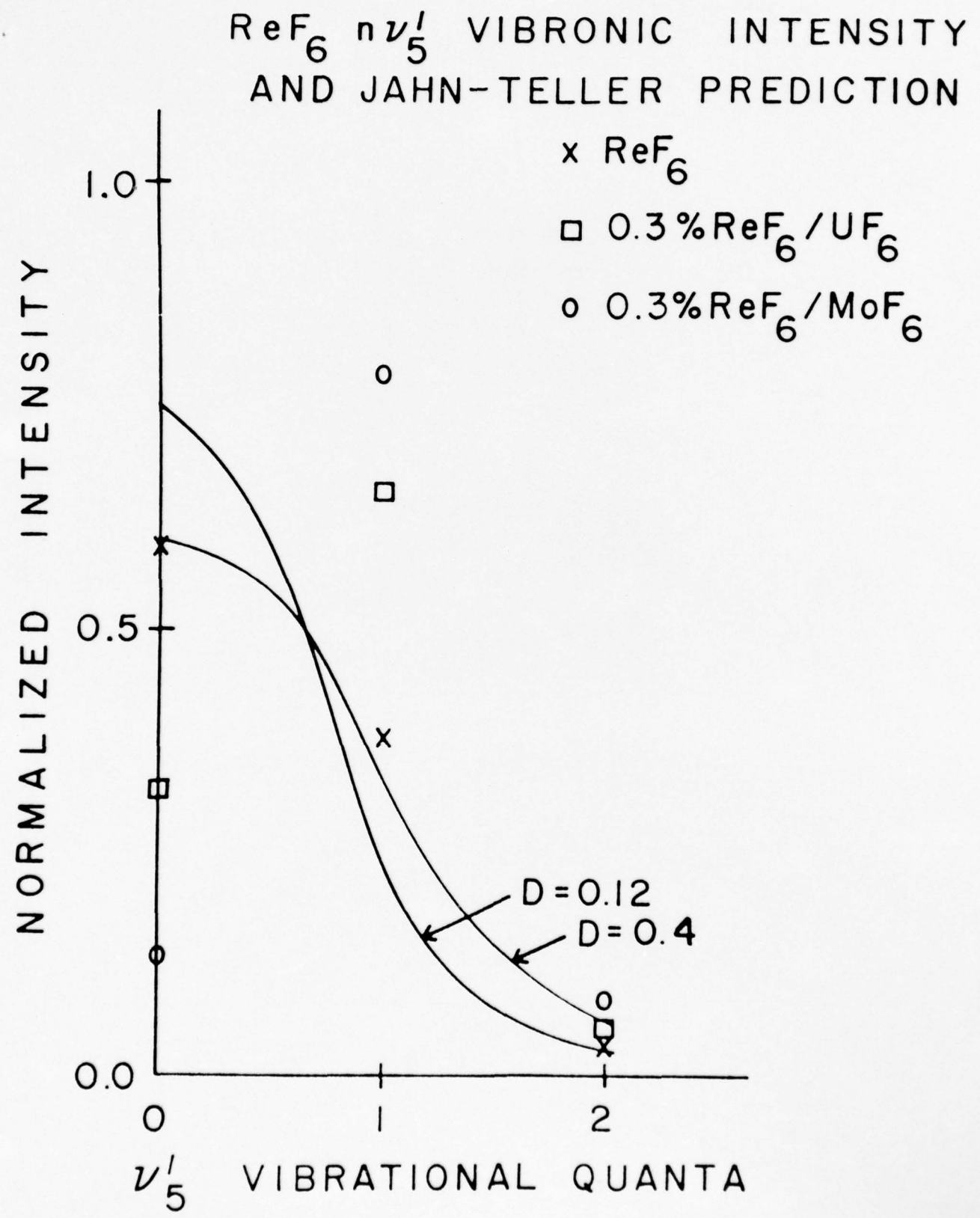
ReF6 nν5' VIBRONIC INTENSITY
AND JAHN-TELLER PREDICTION
x ReF6
□ 0.3%ReF6/UF6
o 0.3%ReF6/MoF6
NORMALIZED INTENSITY
1.0
0.5
0.0
D=0.12
D=0.4
0
1
2
ν5' VIBRATIONAL QUANTA

Figure 10. Predictions of intensities in members of a progression involving a threefold degenerate oscillator, which is both displaced and distorted in an electronic transition, are plotted. Curves occur in sets which encompass ratios of ground state to excited state vibrational frequencies of 0.75 to 1.25. The curves are: (A) $\Delta n = 0$, (B) $\Delta n = +1$, (C) $\Delta n = +2$, (D) the fraction of total progression intensity in first three components. Curves A, B, and C are normalized to unit in those three components to facilitate comparison to Figure 9 data points.

FRANCK-CONDON INTENSITY PREDICTIONS FOR DISPLACED THREE DIMENSIONAL OSCILLATORS

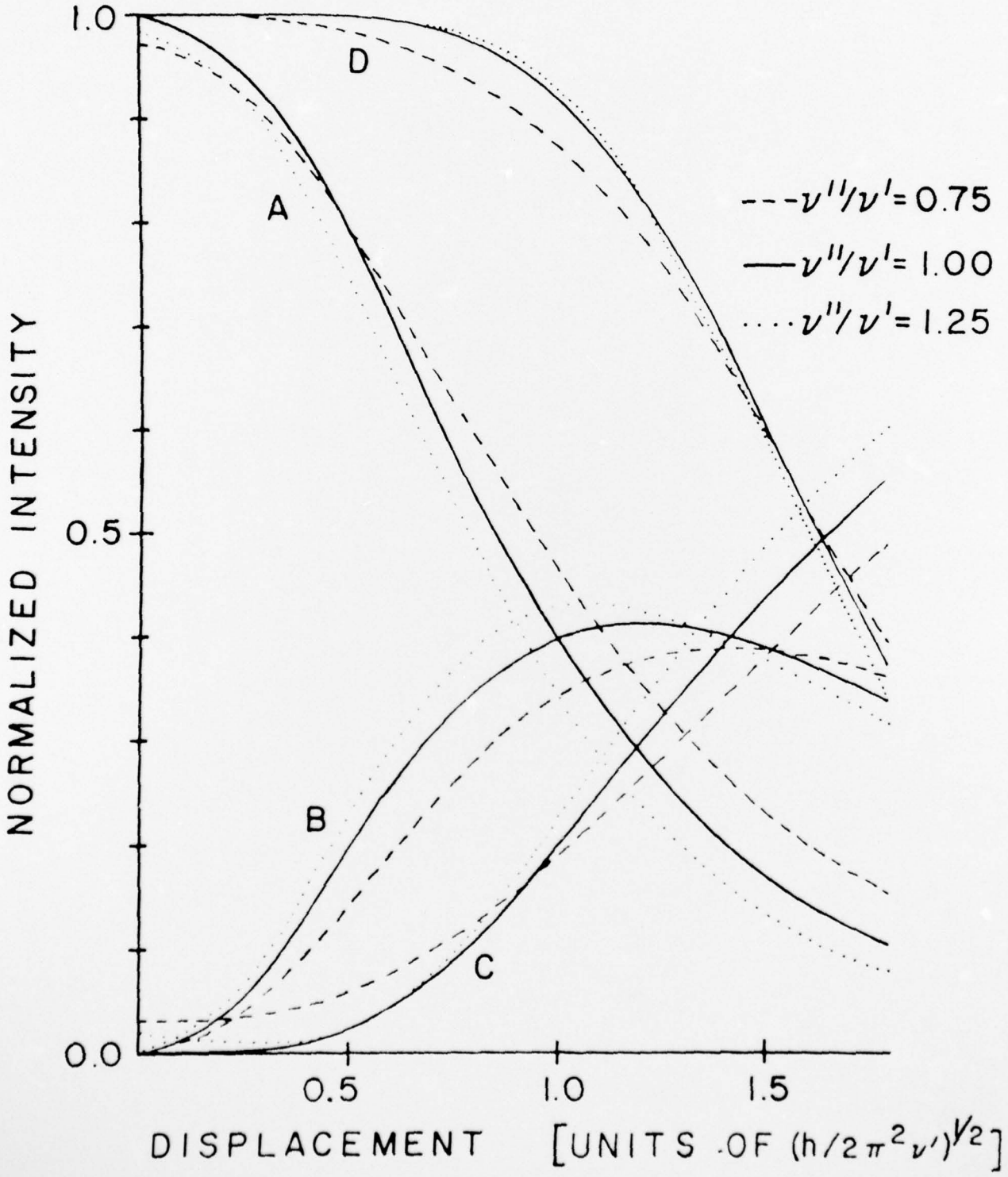

Figure 11. Low resolution Raman spectra of neat ReF_6 crystals are given. Crystals were immersed in liquid nitrogen (A) and superfluid helium (B). The spectra are displayed on logarithmic scales; relative intensities are only qualitatively obvious.

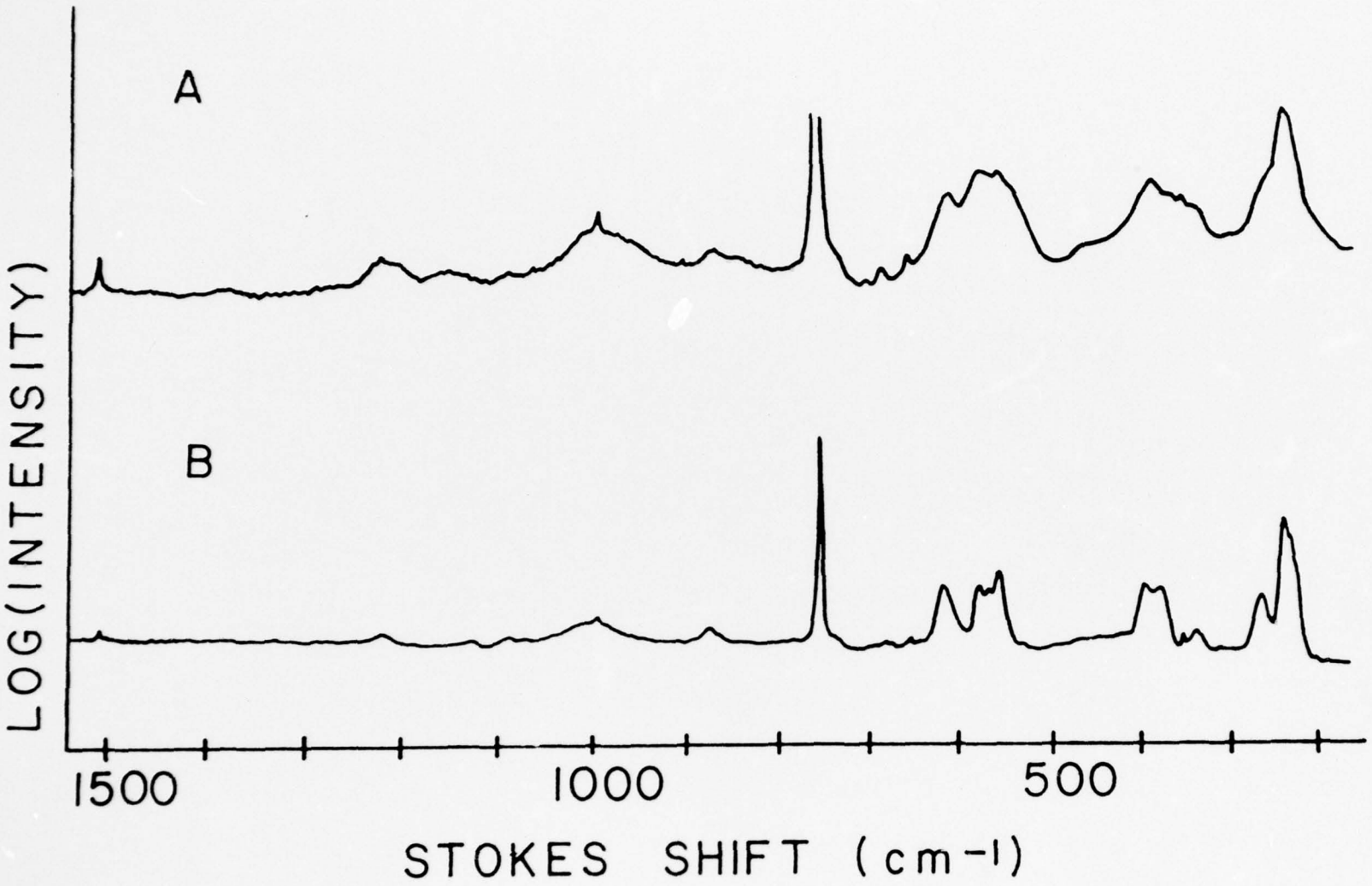
A
B
LOG(INTENSITY)
1500
1000
500
STOKES SHIFT (cm-1)

Figure 12. Schematic representation of the lower vibrational or vibronic energy levels and transitions of a molecule with a low-lying electronic level. This is the energy level system expected for ReF_6 in neat and mixed crystals with $\Delta \sim 25\ cm^{-1}$. See text for discussion.

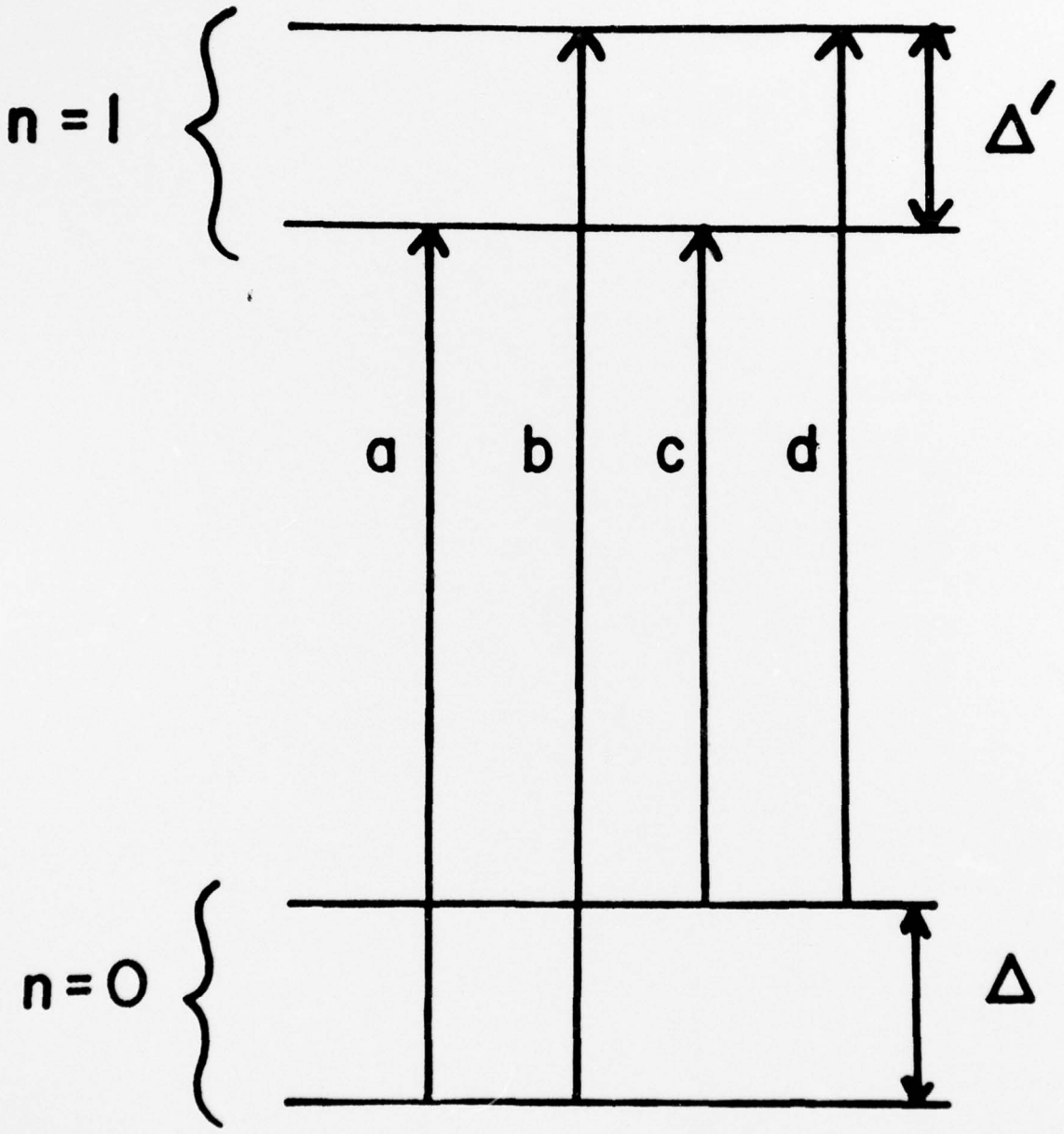
n = 1
Δ′
a
b
c
d
n = 0
Δ

Figure 13. The Raman spectra of the ν_2 (n = 1) vibronic region of ReF_6 in neat and TeF_6 host crystals is presented. The key to the spectra is the following:

(A) Neat ReF_6 crystal in liquid nitrogen

(B) 5 mole percent ReF_6 in TeF_6 mixed crystal in liquid nitrogen

(C) Neat ReF_6 crystal in superfluid helium

(D) 5 mole percent ReF_6 in TeF_6 mixed crystal in superfluid helium

The ~645 cm^{-1} feature of the mixed crystal has been assigned to 2 ν_4 of TeF_6 and nearby weak structure to $\nu_4 + \nu_5$ and 2 ν_5 of TeF_6. The hot bands and temperature dependent shifts are discussed in the text.

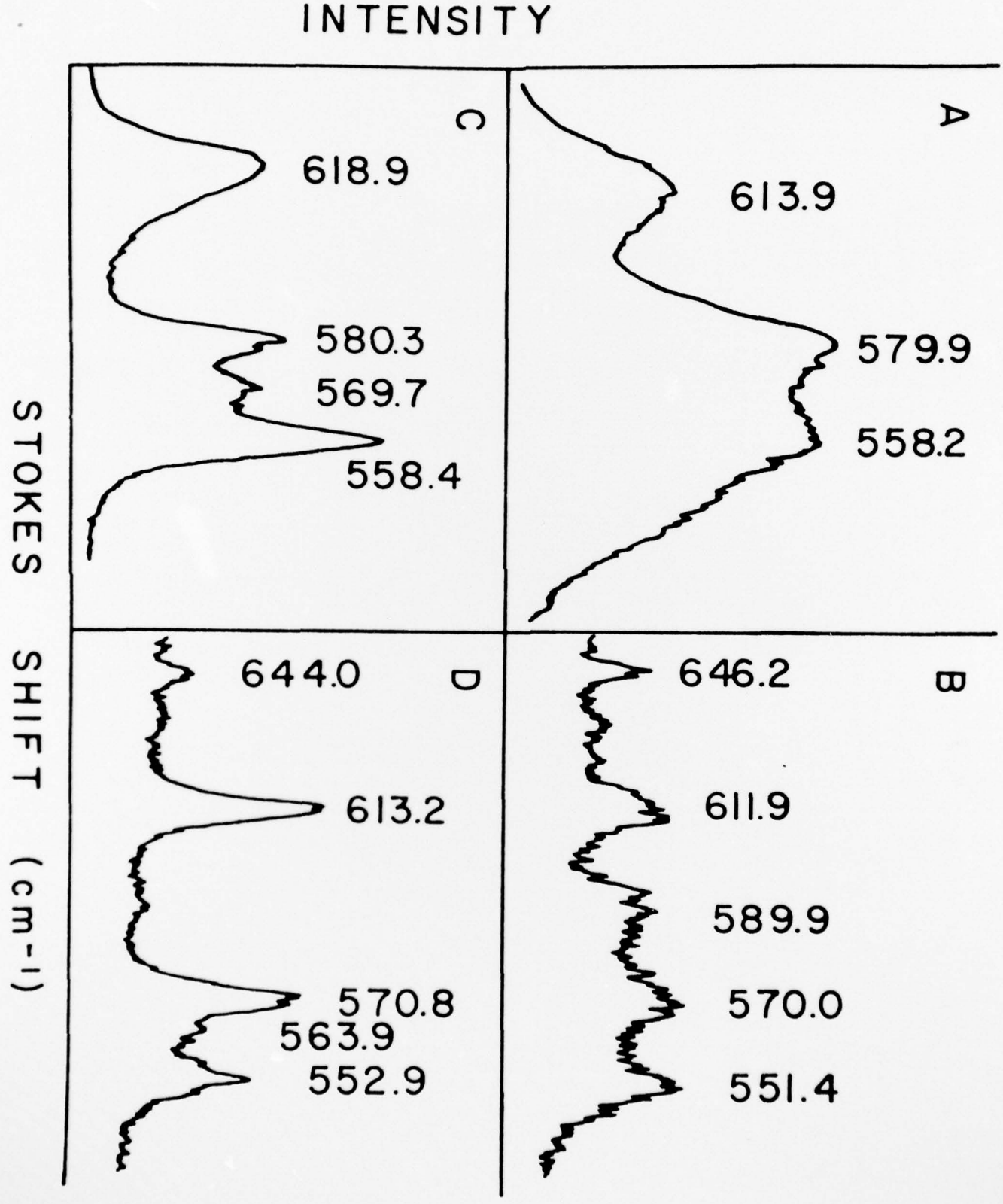
INTENSITY
STOKES SHIFT (cm-1)
C
618.9
580.3
569.7
558.4
A
613.9
579.9
558.2
D
644.0
613.2
570.8
563.9
552.9
B
646.2
611.9
589.9
570.0
551.4

Figure 14. Raman spectra of the $j_5 = 1/2$ region of ReF_6 are presented in neat and TeF_6 host crystals. The key is given in the caption to Figure 13. The weak features around 336 and 351 cm^{-1} in the neat crystals and 338 cm^{-1} in the mixed crystals are assigned to 2 ν_6 of ReF_6. The ~412 cm^{-1} features in the mixed crystal are assigned to 2 ν_6 of TeF_6. The hot band structure, temperature shifts and splittings and broadening are discussed in the text.

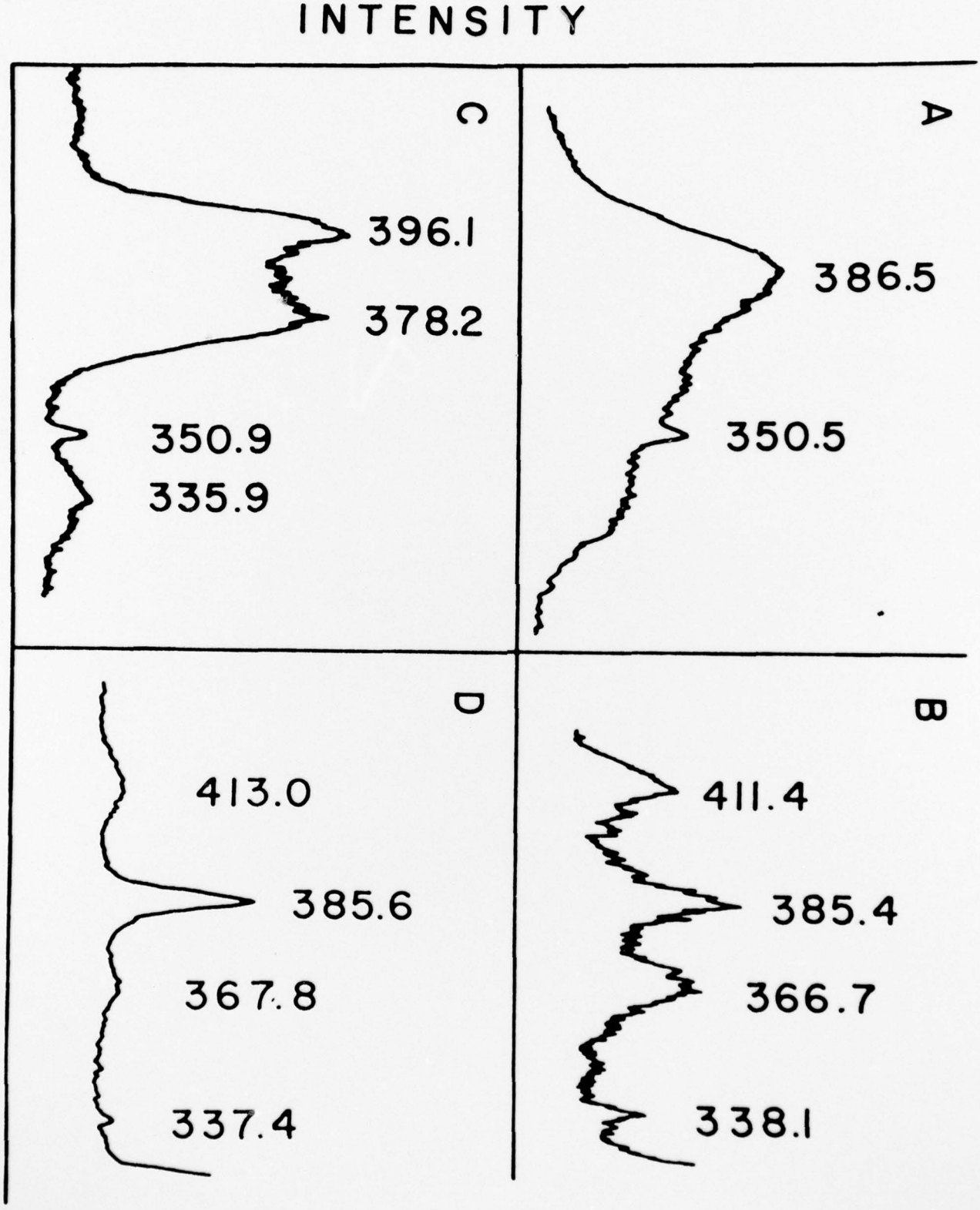
INTENSITY
STOKES SHIFT (cm-1)
C
396.1
378.2
350.9
335.9
A
386.5
350.5
D
413.0
385.6
367.8
337.4
B
411.4
385.4
366.7
338.1

Figure 15. The Raman spectra of the lowest $j_5 = 3/2$ region of ReF_6 is shown in various MF_6 crystals. The key is presented in the caption to Figure 13. The 207 cm^{-1} feature in the mixed crystal has been assigned to ν_6 of TeF_6. The 251 and 247 cm^{-1} features in D and 245 cm^{-1} feature in B have been assigned to ν_4 of ReF_6 although there is some uncertainty in this assignment (see text). The 263 or 257 cm^{-1} features in the neat crystals are assigned similarly. The other details are discussed in the text.

INTENSITY
STOKES SHIFT (cm-1)
A
257
232.4
B
245
228.8
220.6
C
263.3
234.0
227.4
D
250.7
246.8
230.4
219.8
207.2

TECHNICAL REPORT DISTRIBUTION LIST

	No. Copies
Office of Naval Research Arlington, Virginia 22217 Attn: Code 472	2
Office of Naval Research Arlington, Virginia 22217 Attn: Code 102IP	6
ONR Branch Office 536 S. Clark Street Chicago, Illinois 60605 Attn: Dr. George Sandoz	1
ONR Branch Office 715 Broadway New York, New York 10003 Attn: Scientific Dept.	1
ONR Branch Office 1030 East Green Street Pasadena, California 91106 Attn: Dr. R. J. Marcus	1
ONR Branch Office 760 Market Street, Rm. 447 San Francisco, California 94102 Attn: Dr. P. A. Miller	1
ONR Branch Office 495 Summer Street Boston, Massachusetts 02210 Attn: Dr. L. H. Peebles	1
Director, Naval Research Laboratory Washington, D.C. 20390 Attn: Library, Code 2029 (ONRL) Technical Info. Div. Code 6100, 6170	6 1 1
The Asst. Secretary of the Navy (R&D) Department of the Navy Room 4E736, Pentagon Washington, D.C. 20350	1
Commander, Naval Air Systems Command Department of the Navy Washington, D.C. 20360 Attn: Code 310C (H. Rosenwasser)	1

	No. Copi
Defense Documentation Center Building 5, Cameron Station Alexandria, Virginia 22314	12
U.S. Army Research Office P.O. Box 12211 Research Triangle Park, North Carolina 27709 Attn: CRD-AA-IP	
Commander Naval Undersea Research & Development Center San Diego, California 92132 Attn: Technical Library, Code 133	1
Naval Weapons Center China Lake, California 93555 Attn: Head, Chemistry Division	1
Naval Civil Engineering Laboratory Port Hueneme, California 93041 Attn: Mr. W. S. Haynes	1
Professor O. Heinz Department of Physics & Chemistry Naval Postgraduate School Monterey, California 93940	
Dr. A. L. Slafkosky Scientific Advisor Commandant of the Marine Corps (Code RD-1) Washington, D.C. 20380	1

TECHNICAL REPORT DISTRIBUTION LIST

	No. Copies
Dr. M. A. El-Sayed University of California Department of Chemistry Los Angeles, California 90024	1
Dr. M. W. Windsor Washington State University Department of Chemistry Pullman, Washington 99163	
~~Dr. E. R. Bernstein~~ ~~Colorado State University~~ ~~Department of Chemistry~~ ~~Fort Collins, Colorado 80521~~	
Dr. C. A. Heller Naval Weapons Center Code 6059 China Lake, California 93555	1
Dr. G. Jones, II Boston University Department of Chemistry Boston, Massachusetts 02215	
Dr. M. H. Chisholm Chemistry Department Princeton, New Jersey 08540	1
Dr. J. R. MacDonald Code 6110 Chemistry Division Naval Research Laboratory Washington, D.C. 20375	1
Dr. G. B. Schuster Chemistry Department University of Illinois Urbana, Illinois 61801	1
Dr. E. M. Eyring University of Utah Department of Chemistry Salt Lake City, Utah	1
Dr. A. Adamson University of Southern California Department of Chemistry Los Angeles, California 90007	1
Dr. M. S. Wrighton Massachusetts Institute of Technology Department of Chemistry Cambridge, Massachusetts 02139	1